

**SYNTHESIS, CHARACTERIZATION AND BIOLOGICAL  
ACTIVITIES OF ACRIDINE DERIVATIVES AND THEIR  
PLATINUM COMPLEXES**

**NUR AMAJEIDA BINTI ISMAIL**

**FACULTY OF SCIENCE  
UNIVERSITY OF MALAYA  
KUALA LUMPUR**

**2018**

**SYNTHESIS, CHARACTERIZATION AND  
BIOLOGICAL ACTIVITIES OF ACRIDINE  
DERIVATIVES AND THEIR PLATINUM COMPLEXES**

**NUR AMAJEIDA BINTI ISMAIL**

**DISSERTATION SUBMITTED IN FULFILMENT OF  
THE REQUIREMENTS FOR THE DEGREE OF MASTER  
OF SCIENCE**

**DEPARTMENT OF CHEMISTRY  
FACULTY OF SCIENCE  
UNIVERSITY OF MALAYA  
KUALA LUMPUR**

**2018**

**UNIVERSITY OF MALAYA**  
**ORIGINAL LITERARY WORK DECLARATION**

Name of Candidate: **Nur Amajeida binti Ismail**

Matric No: **SGR150059**

Name of Degree: **M.Sc.**

Title of Project Paper/Research Report/Dissertation/Thesis (“this Work”): **Synthesis, Characterization and Biological Activities of Acridine Derivatives and Their Platinum Complexes**

Field of Study: **Inorganic Chemistry**

I do solemnly and sincerely declare that:

- (1) I am the sole author/writer of this Work;
- (2) This Work is original;
- (3) Any use of any work in which copyright exists was done by way of fair dealing and for permitted purposes and any excerpt or extract from, or reference to or reproduction of any copyright work has been disclosed expressly and sufficiently and the title of the Work and its authorship have been acknowledged in this Work;
- (4) I do not have any actual knowledge nor do I ought reasonably to know that the making of this work constitutes an infringement of any copyright work;
- (5) I hereby assign all and every rights in the copyright to this Work to the University of Malaya (“UM”), who henceforth shall be owner of the copyright in this Work and that any reproduction or use in any form or by any means whatsoever is prohibited without the written consent of UM having been first had and obtained;
- (6) I am fully aware that if in the course of making this Work I have infringed any copyright whether intentionally or otherwise, I may be subject to legal action or any other action as may be determined by UM.

Candidate’s Signature

Date:

Subscribed and solemnly declared before,

Witness’s Signature

Date:

Name:

Designation:

# SYNTHESIS, CHARACTERIZATION AND BIOLOGICAL ACTIVITIES OF ACRIDINE DERIVATIVES AND THEIR PLATINUM COMPLEXES

## ABSTRACT

New compounds have been successfully synthesized. The chemical structure of all synthesized compounds, were characterized by using elemental analysis CHN, FTIR,  $^1\text{H}$  NMR,  $^{13}\text{C}$  NMR, APT NMR, Thermal gravimetric analysis (TGA) and single X-ray crystallography. Ligands were derived from acridine and various substituent of aniline, then reacted with Pt(II) salt to form the complexes. The ligand consists of four aromatic rings which three of it are in the form of acridine parent skeleton structure and another one is the substituent of aniline. The synthesized ligands were coordinated to the platinum salt *via* nitrogen atom, in which the core is in the turn of tetrahedral with either chloride or DMSO attached to it. The acridine acts as a neutral N-monodentate ligand. The reaction of ligands with Pt(II) salt in 1:1 (ligand/metal) molar ratio afforded complexes of Pt G3, Pt G4 and Pt G7. In the presence of sodium acetate, the reaction of acridine with  $\text{PtCl}_2\text{DMSO}_2$  remain in base condition to form acridine platinum complexes. The acridine derivatives and its platinum complexes were found to have a significant cytotoxicity value towards three cancer cell lines, namely MCF-7, HL60 and HT29 but not toward the normal liver WRL-68 cell line. The biological activities have been conducted for all of the synthesized compounds, through MTT cytotoxicity assay and selected compound on acute toxicity. All compounds were significantly inhibited the proliferation of MCF-7, HL60 and HT29 cells that was shown in the cytotoxicity assay ( $\text{IC}_{50}$  value). Doxorubicin was used as a positive control. Hence the synthesized compounds are promising to be the future drugs as they are highly potent to induce apoptosis in MCF-7 or HL60 cells *via* intrinsic mitochondrial pathway.

**Keywords:** acridine; heterocycle; acute toxicity; antiproliferative

# SENTESIS, PENCIRIAN DAN AKTIVITI BIOLOGI TERHADAP TERBITAN AKRIDIN DAN KOMPLEKS PLATINUMNYA

## ABSTRAK

Beberapa sebatian baru telah berjaya disintesis. Struktur kimia bagi semua sebatian yang disintesis telah dicirikan dengan menggunakan analisis unsur CHN, FTIR,  $^1\text{H}$  NMR,  $^{13}\text{C}$  NMR, APT NMR, analisis gravimetrik terma (TGA) and kristalografi hablur tunggal sinaran-X. Ligan telah direkabentuk daripada akridin dan pelbagai penyambungan anilin, seterusnya tindakbalas dengan garam Pt(II) bagi membentuk kompleks. Ligan mengandungi empat gelang aromatik yang dimana tiga daripadanya adalah daripada struktur utama akridin, manakala satu lagi daripada penyambungan anilin. Koordinasi platinum berlaku pada atom nitrogen daripada ligan, yang terasnya terdiri daripada geometri tetrahedral dengan pengkoordinasian sama ada klorida atau DMSO. Akridin bertindak sebagai ligan N-monodentat neutral. Tindakbalas dengan garam Pt(II) dalam nisbah 1:1 (ligan:logam) membentuk kompleks Pt G3, Pt G4 dan Pt G7. Natrium asetat digunakan dalam tindakbalas akridin dengan  $\text{PtCl}_2\text{DMSO}_2$  untuk mengekalkan keadaan beralkali bagi pembentukan kompleks platinum. Terbitan akridin dan kompleks platinumnya mempunyai nilai sitotoksiti terhadap tiga sel kanser, terdiri daripada MCF-7, HL60 and HT29 tetapi bukan terhadap sel hati WRL-68 yang normal. Aktiviti biologi telah dijalankan keatas semua sebatian yang disintesis, melalui ujian sitotoksiti MTT dan ujian ketoksikan akut pula untuk sebatian terpilih sahaja. Semua sebatian dapat merencat percambahan sel MCF-7, HL60 dan HT29 yang telah ditunjukkan dalam ujian sitotoksiti MTT (nilai  $\text{IC}_{50}$ ). Doksorubisin telah digunakan sebagai kawalan positif. Kesimpulannya, semua sebatian yang disintesis mempunyai potensi sebagai ubat pada masa hadapan memandangkan aktiviti apoptosis yang berkesan di dalam sel MCF-7 atau HL60 melalui jalur mitokondria intrinsik.

**Kata kunci:** akridin; heterosiklik; ujian ketoksikan akut; antiproliferatif

## ACKNOWLEDGEMENTS

First and foremost, praise only to Allah, the most gracious and merciful, for His blessing that I am able to complete this thesis.

I would like to express my sincere appreciation to my supervisor, Dr. Rozie Sarip for her continuous support patience and knowledge that benefited me in the completing of this study; which would not be possible without her persistent guidance and assistance. And also I would like to thank Prof. Dr. Hapipah Mohd Ali for being a constant source of motivation and excellent guide during my studies.

I want to thank the staff members of Chemistry Department, University of Malaya for their kind help in assessing the research facilities during carrying my lab work. I would also love to thank to my lab mates and friends for their assistance and motivation.

Last but not least, the greatest appreciation is dedicated to my family to whom I am indebted the most. The tender love, care and support are the reason I become what I am today.

## TABLE OF CONTENTS

ABSTRACT.....	iii
ABSTRAK.....	iv
ACKNOWLEDGEMENTS.....	v
TABLE OF CONTENTS.....	vi
LIST OF FIGURES.....	ix
LIST OF SCHEMES.....	x
LIST OF TABLES.....	xi
LIST OF SYMBOLS AND ABBREVIATIONS.....	xii
LIST OF APPENDICES.....	xv
<b>CHAPTER 1: INTRODUCTION.....</b>	<b>1</b>
1.1 Introduction.....	1
1.1.1 Bernthsen Acridine Synthesis.....	2
1.1.2 Friedländer Synthesis.....	2
1.1.3 Ullmann Reaction.....	3
1.2 The objective of study.....	6
<b>CHAPTER 2: LITERATURE REVIEW.....</b>	<b>7</b>
2.1 Acridine.....	7
2.2 Platinum complexes.....	9
2.3 The biological important of acridine and its derivatives.....	10
<b>CHAPTER 3: METHODOLOGY.....</b>	<b>12</b>
3.1 Materials and Instrumentation.....	12
3.2 General preparation of ligands and their complexes.....	13

3.3	Preparation of the precursors .....	15
3.3.1	Synthesis of 2-(phenylamino)benzoic acid, G1 .....	15
3.3.2	Synthesis of 9-chloroacridine, G2 .....	16
3.4	Preparation of ligands and Platinum complexes.....	17
3.4.1	Synthesis of N-phenylacridin-9-amine, G3 .....	17
3.4.2	Synthesis of (N-phenylacridin-9-amine)cis-dichloro(dimethylsulfoxide)- platinum(II), Pt G3 .....	18
3.4.3	Synthesis of N-(3,5-dimethoxyphenyl)acridin-9-amine, G4.....	19
3.4.4	Synthesis of (N-(3,5-dimethoxyphenyl)acridin-9-amine) cis-dichloro (dimethylsulfoxide) platinum(II), Pt G4 .....	20
3.4.5	Synthesis of N-(4-fluorophenyl)acridin-9-amine, G7 .....	21
3.4.6	Synthesis of (N-(4-fluorophenyl) acridin-9-amine) cis-dichloro (dimethylsulfoxide) platinum(II) acridine, Pt G7.....	22
3.5	Biological activity.....	23
3.5.1	In vitro cytotoxicity Assay .....	23
3.5.2	Acute Toxicity Test for G4.....	24
3.6	Animal	24
3.7	Experimental Animals .....	24
3.8	Assessment of kidney and liver functions .....	25
3.9	Assessment of lipid profile .....	25
3.10	Histopathological examinations.....	26
3.11	Measurement of lipid peroxidation.....	26
3.12	Measurement of tissues glutathione.....	26
3.13	Statistical analysis.....	27
<b>CHAPTER 4: RESULTS AND DISCUSSION .....</b>		<b>28</b>
4.1	Mechanism of action for synthesis of acridine derivatives and their complexes ..	29

4.2	General and spectroscopic characterization ligands and complexes of acridine derivatives.....	33
4.3	IR Spectral Data.....	35
4.4	<sup>1</sup> H NMR Spectral Data .....	38
4.5	<sup>13</sup> C NMR Spectral Data .....	42
4.6	X-ray Crystallographic Study .....	46
4.6.1	Crystal structure of G4 .....	46
4.6.2	Crystal structure of Pt G3 .....	49
4.6.3	Crystal structure of Pt G4.....	50
4.7	Biological activity.....	56
4.7.1	Anti-proliferative activity of compounds .....	56
4.7.2	General acute toxicity observation for G4.....	57
4.7.3	Serum biochemical parameters .....	59
4.7.4	Histopathological evaluation.....	60
	<b>CHAPTER 5: CONCLUSION.....</b>	<b>61</b>
5.1	Future work.....	62
	REFERENCES.....	63
	LIST OF PUBLICATIONS AND PAPER PRESENTED .....	72
	APPENDIX.....	74

## LIST OF FIGURES

Figure 1.1: Bernthsen Acridine Synthesis.....	2
Figure 1.2: Friedländer Synthesis .....	3
Figure 1.3: Ullmann Reaction.....	3
Figure 1.4: Synthesis 2-Phenylamino benzoic acid by Ullmann reaction .....	4
Figure 2.1: The similarity skeleton of acridine and anthracene.....	7
Figure 2.2: The skeleton of acridine, xanthone and thioxanthone.....	8
Figure 2.3: Two tautomeric form of 9-aminoaniline .....	9
Figure 4.1: Comparison of IR spectra between ligand G3 and Pt (II) complex Pt G3 ...	37
Figure 4.2: <sup>1</sup> H NMR spectrum of N-phenylacridin-9-amine, G3 (400 MHz, chloroform-D) .....	40
Figure 4.3: <sup>1</sup> H NMR spectrum of (N-phenylacridin-9-amine) cisdichloro (dimethylsulfoxide) platinum(II), Pt G3 (400 MHz, DMSO <sub>d</sub> <sub>6</sub> .....	41
Figure 4.4: <sup>13</sup> C NMR spectrum of N-phenylacridin-9-amine, G3 (400 MHz, chloroform-D) .....	44
Figure 4.5: <sup>13</sup> C NMR spectrum of (N-phenylacridin-9-amine) cis-dichloro (dimethylsulfoxide) platinum(II), Pt G3 (400 MHz, DMSO <i>d</i> <sub>6</sub> .....	45
Figure 4.6: The ORTEP diagram of G4, showing 50% probability displacement ellipsoids and the atom-numbering scheme .....	48
Figure 4.7: The packing of G4 viewed down to the b axis .....	49
Figure 4.8: The crystal structure of platinum complex, Pt G3 ORTEP.....	50
Figure 4.9: The crystal structure of platinum complex, Pt G4 ORTEP.....	51
Figure 4.10: The TGA data of G7.....	55
Figure 4.11: The TGA data of Pt G7.....	55
Figure 4.12: Effect of G4 compound on histological sections of the liver and kidney in rats. (A, B) Rats treated with vehicle. (C, D) Rats treated with 500 mg/kg of G4. (E, F) Rats treated with 1000 mg/kg of G4. (H &E stain, 20× magnifications) .....	60

## LIST OF SCHEMES

Scheme 3.1: General overview to produce derivatives of acridine. Reagents and conditions: (a) K <sub>2</sub> CO <sub>3</sub> , Cu, CuI, DMF, 130 °C; (b) POCl <sub>3</sub> , 138 °C, (c) K <sub>2</sub> CO <sub>3</sub> , KI, absolute ethanol, 78 °C; (d) PtCl <sub>2</sub> DMSO <sub>2</sub> , NaOAc, methanol:toluene (2:1), 65 °C; (e) PtCl <sub>2</sub> DMSO <sub>2</sub> , NaOAc, ethanol .....	14
Scheme 3.2: Synthesis of 2-(phenylamino)benzoic acid, G1 .....	15
Scheme 3.3: Synthesis of 9-chloroacridine, G2 .....	16
Scheme 3.4: Synthesis of N-phenylacridin-9-amine, G3 .....	17
Scheme 3.5: Synthesis of (N-phenylacridin-9-amine)cis-dichloro(dimethylsulfoxide)-platinum(II), Pt G3 .....	18
Scheme 3.6: Synthesis of N-(3,5-dimethoxyphenyl)acridin-9-amine, G4 .....	19
Scheme 3.7: Synthesis of (N-(3,5-dimethoxyphenyl) acridin-9-amine) cis-dichloro(dimethylsulfoxide) platinum(II), Pt G4 .....	20
Scheme 3.8: Synthesis of N-(4-fluorophenyl)acridin-9-amine, G7 .....	21
Scheme 3.9: Synthesis (N-(4-fluorophenyl) acridin-9-amine) cis-dichloro (dimethylsulfoxide) platinum(II) acridine, Pt G7 .....	22
Scheme 4.1: Mechanism of Ullmann reaction .....	29
Scheme 4.2: Mechanism of 2-phenylamino benzoic acid, G1 .....	29
Scheme 4.3: Mechanism of cyclization to form 9-chloroacridine, G2 .....	30
Scheme 4.4: Mechanism of the synthesis acridine derivatives .....	31
Scheme 4.5: Mechanism of platinum complexes of Pt G3 and Pt G7 .....	32
Scheme 4.6: Mechanism of platinum complex of Pt G4 .....	33

## LIST OF TABLES

Table 4.1: Physical properties and analytical data of acridine derivatives and their Pt (II) complexes.....	34
Table 4.2: Selected IR spectral data of acridine derivatives and their platinum (II) complexes.....	36
Table 4.3: Selected <sup>1</sup> H NMR data of acridine derivatives and their platinum (II) complexes.....	39
Table 4.4: Selected <sup>13</sup> C NMR Data of acridine derivatives and their platinum (II) complexes.....	43
Table 4.5: Crystal data and structure refinement for G4.....	47
Table 4.6: Selected bond length (Å) and angles (°).....	48
Table 4.7: Selected bond length (Å) and bond angles (°) for the Pt G3 and Pt G4 complexes.....	52
Table 4.8: Crystal data and structure refinement of Pt G3 and Pt G4 complexes.....	53
Table 4.9: The theoretical and the experimental of remaining product after decomposition process.....	54
Table 4.10: Cytotoxicity effect of G3, G4, G7, Pt G3, Pt G4 and Pt G7.....	57
Table 4.11: Serum biochemical data for male and female mice orally administered G4 at different concentration for 14 days. ....	58
Table 4.12: The effect of G4 on triglyceride, total cholesterol, HDL cholesterol and LDL cholesterol. ....	59

## LIST OF SYMBOLS AND ABBREVIATIONS

Å	:	Angstrom
abs. EtOH	:	Absolute ethanol
ALP	:	Alkaline phosphate
ALT	:	Serum alanine aminotransferase
AO	:	Acridine Orange
APT NMR	:	<sup>13</sup> C-Attached Proton Test
br	:	Broad
C	:	Carbon
CDCl <sub>3</sub>	:	Deuterated chloroform
CHN	:	Carbon, Hydrogen and Nitrogen elemental analysis
Cisplatin	:	<i>Cis</i> -diamminedichloroplatinum (II)
Cl	:	Chloride
<sup>13</sup> C NMR	:	<sup>13</sup> C Nuclear Magnetic Resonance
° C	:	Degree Celsius
d	:	Doublet
dd	:	Doublet doublet
ddt	:	Doublet doublet triplet
DMF	:	Dimethylformamide
DMSO	:	Dimethyl sulfoxide
DMSO- <i>d</i> <sub>6</sub>	:	Deuterated dimethyl sulfoxide- <i>d</i> <sub>6</sub>
DNA	:	Deoxyribonucleic acid
δ	:	Chemical shifts
F	:	Fluorine
FTIR	:	Fourier-transform infrared

g	:	Gram
GGT	:	Gamma-glutamyl transferase
GSH	:	Glutathione
h	:	Hour
Hz	:	Hertz
HCL	:	Hydrochloric acid
HDL	:	High-density Lipoprotein
HL60	:	Leukemia Cancer Cell line
HT29	:	Colon Cancer Cell Line
<sup>1</sup> H NMR	:	<sup>1</sup> H Nuclear Magnetic Resonance
IC <sub>50</sub>	:	Half Maximal Inhibitory Concentration
<i>J</i>	:	Coupling Constant
MCF – 7	:	Breast Cancer Cell Line
MDA	:	Malondialdehyde
MeOH	:	Methanol
MHz	:	Megahertz
m.p	:	Melting Point
MTT	:	3-(4,5-dimethylthiazol-2-yl)-2,5-diphenyltetrazolium bromide
N	:	Nitrogen
O	:	Oxygen
Pt	:	Platinum
ppm	:	Parts per million
POCl <sub>3</sub>	:	Phosphorus Oxychloride
PtCl <sub>2</sub> (DMSO) <sub>2</sub>	:	<i>Cis</i> -dichloro(dimethylsulfoxide)-platinum(II) salt
RNA	:	Ribonucleic acid

s	:	Singlet
S	:	Sulphur
T	:	Triplet
TBA	:	2-thiobarbituric acid
TGA	:	Thermo Gravimetric Analysis
TMS	:	Tetramethylsilane
TLC	:	Thin Layer Chromatography
$\mu_{\text{eff}}$	:	Magnetic Moment
WRL – 68	:	Hepatic human cell line

University of Malaya

## LIST OF APPENDICES

<b>Appendix A:</b> IR spectra of G1.....	74
<b>Appendix B:</b> IR spectra of G2.....	75
<b>Appendix C:</b> IR spectra of G4.....	76
<b>Appendix D:</b> IR spectra of Pt G4.....	77
<b>Appendix E:</b> IR spectra of G7.....	78
<b>Appendix F:</b> IR spectra of Pt G7.....	79
<b>Appendix G:</b> <sup>1</sup> H NMR spectrum of 2-(phenylamino)benzoic acid, G1 (400 MHz, chloroform-D) .....	80
<b>Appendix H:</b> <sup>1</sup> H NMR spectrum of 9-chloroacridine G2 (400 MHz, chloroform-D) .....	81
<b>Appendix I:</b> <sup>1</sup> H NMR spectrum of N-(3,5-dimethoxyphenyl)acridin-9-amine G4 (400 MHz, chloroform-D) .....	82
<b>Appendix J:</b> <sup>1</sup> H NMR spectrum of (N-(3,5-dimethoxyphenyl) acridin-9-amine) cis-dichloro (dimethylsulfoxide) platinum(II) Pt G4 (400 MHz, DMSO <i>d</i> <sub>6</sub> ) .....	83
<b>Appendix K:</b> <sup>1</sup> H NMR spectrum of N-(4-fluorophenyl)acridin-9-amine G7 (400 MHz, DMSO <i>d</i> <sub>6</sub> ) .....	84
<b>Appendix L:</b> <sup>1</sup> H NMR spectrum of (N-(4-fluorophenyl) acridin-9-amine) cis-dichloro (dimethylsulfoxide) platinum(II) acridine Pt G7 (400 MHz, DMSO <i>d</i> <sub>6</sub> ) .....	85
<b>Appendix M:</b> <sup>13</sup> C NMR spectrum of 2-(phenylamino)benzoic acid, G1 (400 MHz, chloroform-D).....	86
<b>Appendix N:</b> <sup>13</sup> C NMR spectrum of 9-chloroacridine G2 (400 MHz, chloroform-D) .....	87

<b>Appendix O:</b> $^{13}\text{C}$ NMR spectrum of N-(3,5-dimethoxyphenyl)acridin-9-amine G4 (400 MHz, chloroform-D) .....	88
<b>Appendix P:</b> $^{13}\text{C}$ NMR spectrum of (N-(3,5-dimethoxyphenyl) acridin-9-amine) cis-dichloro (dimethylsulfoxide) platinum(II) Pt G4 (400 MHz, DMSO $d_6$ ) .....	89
<b>Appendix Q:</b> $^{13}\text{C}$ NMR spectrum of N-(4-fluorophenyl)acridin-9-amine G7 (400 MHz, DMSO $d_6$ ).....	90
<b>Appendix R:</b> $^{13}\text{C}$ NMR spectrum of (N-(4-fluorophenyl) acridin-9-amine) cis-dichloro (dimethylsulfoxide) platinum(II) acridine Pt G7 (400 MHz, DMSO $d_6$ ).....	91
<b>Appendix S:</b> The crystal structure of platinum complex, G4.....	92
<b>Appendix T:</b> The crystal structure of platinum complex, Pt G4.....	92
<b>Appendix U:</b> The crystal structure of platinum complex, Pt G3.....	93
<b>Appendix V:</b> The TGA data of G3.....	94
<b>Appendix W:</b> The TGA data of Pt G3.....	95
<b>Appendix X:</b> The TGA data of G4.....	96
<b>Appendix Y:</b> The TGA data of Pt G4.....	97

## CHAPTER 1: INTRODUCTION

### 1.1 Introduction

Acridine is a class of organic compounds known as  $\pi$ -electron-deficient heterocycles that possess a number of unique chemical and physical properties (Korth et al., 2001; Kumar et al., 2015). Acridine structure consist of a nitrogen and aromatic rings with the formula of  $C_{13}H_9N$ . The present of aromatic ring like the aza-aromatic compounds will show the potential of compound toward the biological and physical application. The aromatic ring have their own ability to contribute its behavior to transfer an electron either donating the electron or withdrawing the electron to form the stable formation of molecule. Then, the aromatic ring also known as a bulky compound which somehow good in the metallation reaction to form complex. The chelating agents also one of the factor that exists in acridine compound. The nitrogen atom in acridine act as N-donor ligand, which has a high tendency to form the cyclometallate compounds (Aitken et al., 2007; Budzisz et al., 2007; Mochida et al., 2006). The behavior of nitrogen atom as a heteroatom will enhance the chelate between metal and acridine.

Nowdays, the modification of acridine by metallation is an interesting field for researchers in their quest to discover new potent anticancer agents (Ding et al., 2014; Hernán-Gómez et al., 2015; Souibgui et al., 2014). Most of researcher were focus on these compounds due to the unique of its skeleton. There are many ways to synthesis the skeleton of acridine namely; Bernthsen acridine synthesis, Friedlander synthesis and Ullman reaction (Garnier et al., 2018; Godino-Ojer et al., 2018; Kim et al., 2018; Saini & Dharawath, 2018).

### 1.1.1 Berntsen Acridine Synthesis

The Berntsen reaction (**Figure 1.1**), one of the earliest used for the synthesis of acridines, (**II**) consists of heating a mixture of an aromatic or aliphatic carboxylic acid (acid anhydride) with a diphenylamine (**I**) and zinc chloride at 200-270 °C for about twenty hours (Popp, 1962).

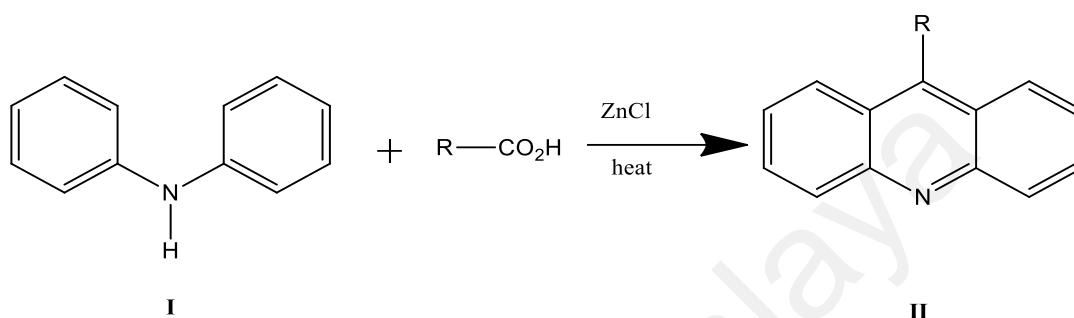


**Figure 1.1:** Berntsen Acridine Synthesis

In some cases, the Berntsen reaction needs polyphosphoric acid as catalyst (Das & Thakur, 2011). For example, a reaction of diphenylamine with benzoic acid in polyphosphoric acid for 15 minutes at 200 °C resulting in the formation of acridine compound. However, the reaction of *p*-nitrobenzoic acid with zinc chloride to form acridine is not as successful that is due to the existence of nitro- substituent. The nitrogen atom owned by the nitro group will delocalized the electrons to form the stable condition affecting the acridine.

### 1.1.2 Friedländer Synthesis

Another synthetic way to synthesis acridine is by the reaction of ketone with 2-aminobenzaldehydes, catalyzed by trifluoroacetic acid, iodine and toluene sulfonic acid (**Figure 1.2**). The reaction was named after a German chemist, Paul Friedländer (1857-1923). The method involving an acid- or base-catalyzed condensation reaction followed by the cyclodehydration between substituted aromatic aldehyde and ketone which containing  $\alpha$ -methylene group (Jia et al., 2006; Teimouri & Chermahini, 2016). Hence, this synthetic pathway was proven to be the most simple method to synthesis acridine or poly substituted quinolones (Cheng & Yan, 2004; Wang, 2010).

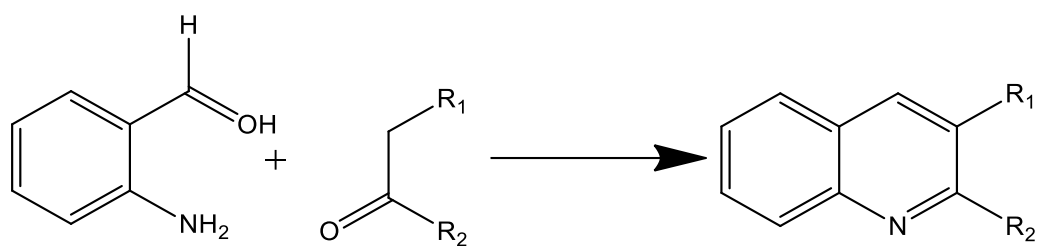


**Figure 1.2:** Friedländer Synthesis

### 1.1.3 Ullmann Reaction

A coupling reaction between aryl halides and copper also known as Ullmann coupling (**Figure 1.3**) (Sambiagio et al., 2014). There are two important mechanism of Ullmann reaction; first, a radical mechanism when a single electron transferred from the copper metal to the alkyl halide to form an aryl radical. Then the final biaryl products were formed when two aryl react together. Second, a mechanism starts with an oxidative addition of copper to aryl halide followed by single electron transfer to form an organocuprate reagent. Next, the organocuprate performs another oxidative addition on aryl halide. Lastly, the final biaryl product formed after the reductive elimination (Mondal, 2016). **Figure 1.4** shows the synthetic pathway of 2-phenylamino benzoic acid *via* Ullmann reaction.

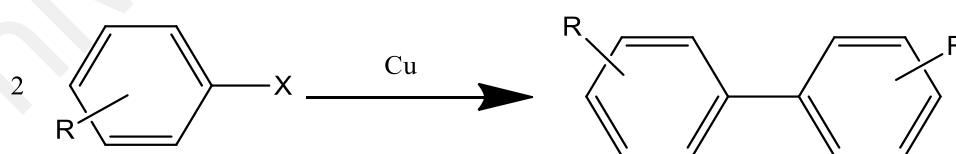


**Figure 1.3:** Ullmann Reaction

The unique of acridine skeleton either in acid or base form will contribute to many applications. In physical applications, acridine orange (AO) (Dai et al., 2016; Kawasaki et al., 2017; Rubio-Pons et al., 2001; Zhang et al., 2015) has been used as the detection of tumors, metastases, and residual disease after surgical excision (Gensicka-Kowalewska et al., 2017; Mondek et al., 2014). Acridine orange is a cell permeant nucleic acid binding dye which can emits green fluorescence when it bound to DNA. While, the red fluorescence emits when bound to DNA or RNA. Due to this characteristic, the acridine orange is useful in cell-cyle studies. Meanwhile, acridine yellow has been used as a dye-like biomolecule (Fahrenholtz et al., 2016; Mukherjee et al., 2016) in numerous photosensitizer studies. Others usage of acridine such as in solar cell production (Liu et al., 2016), in which acridine yellow is involved in the synthesis of TiO<sub>2</sub> films containing nanosized semiconductor particles. While in the biological activity, acridine can primarily be attributed to its core structure which are benzene ring and either –NHCH<sub>2</sub>- or –NHCH<sub>2</sub>CH<sub>2</sub>- groups. Other substituents that attach to acridine (Borovlev et al., 2016; Sondhi et al., 2013), are proven to be able to enhance the biological potency of acridine and reduce its side effects following interaction with DNA (Bacherikov et al., 2005; Di Giorgio et al., 2008; Ketron et al., 2012; Loza-Mejía et al., 2009).

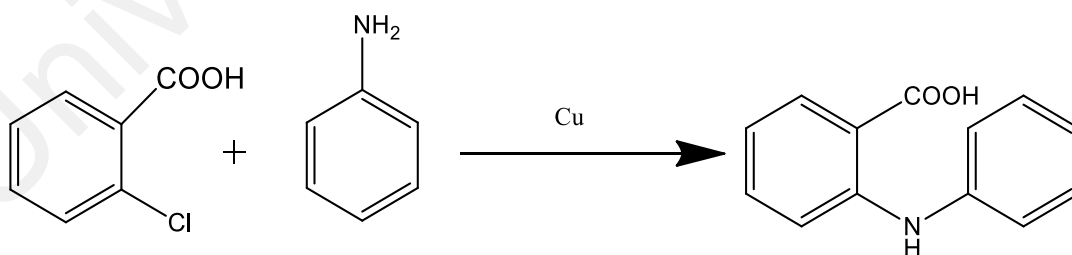


**Figure 1.4:** Synthesis 2-Phenylamino benzoic acid by Ullmann reaction

Acridine also reported to act as chemotherapeutic drugs especially as antileukemic agent (Gao et al., 1998; Janočková et al., 2015). A polycyclic aromatic compound of acridine with the  $\pi$ -conjugate structure will enhance intercalate into DNA. Furthermore, amsacrine (m-AMSA), an acridine derivative, was proven to be the first known DNA-intercalating agent, or topoisomerase II inhibitor (Almeida et al., 2016; Janovec et al., 2011; Lang et al., 2013). Acridine also possesses a wide range of other biological activities, which include antibacterial (Benoit et al., 2014; Wainwright, 2001), trypanocidal (Gamage et al., 1997), antimalarial (Prajapati et al., 2017; Valdés, 2011) and antiparasitic activities (Caffrey et al., 2007).

## 1.2 The objective of study

The objectives of this study are:

1. To synthesis a series of acridine derivatives.
2. To synthesis platinum complexes using the synthesized acridine.
3. To elucidate the structure of acridine derivatives and platinum complexes by using various spectroscopic techniques, single crystal X-ray, CHN and TGA analyses.
4. To investigate their biological properties of the ligands and platinum complexes obtained.

This thesis is divided into five chapters. Chapter 1; an introduction of general acridine derivatives and the type of synthesis skeleton of acridine. Chapter 2 is about the literature review of acridine properties and the potential of substituents and metal toward acridine. Then, some information about the general introduction of biological application especially anticancer with acridine derivatives. In Chapter 3 will describes detail about the methods used to synthesize acridine derivatives and its complexes. The procedures of the MTT test and acute toxicity test toward mice is also outlined in this chapter. Chapter 4 consists of the results and discussion of the studied compounds. The six compounds were characterized by FTIR, NMR, CHN analyses and X-ray crystallography. The reaction mechanism of acridine compound is also discussed in this chapter. Lastly, Chapter 5 summarized the general conclusions and future work about this research.

## CHAPTER 2: LITERATURE REVIEW

### 2.1 Acridine

The acridines represent an important group that is structurally related to anthracene as shown in **Figure 2.1**. This organic molecule have similarity to the acridine skeleton. Acridine consist of three parent rings which one of the central CH group being replaced by nitrogen atom. In room temperature, acridine is mildly basic and form in pale yellow in crystal condition or colorless solid precipitate. Acridine is one of the agents with interest in the field of photodynamic therapy and biological activity (Kumar et al., 2017; Sondhi et al., 2010). Other usage of acridine as in biological field for example, the derivatives of 9-anilinoacridine was shown to inhibit *P. falciparum* growth in culture and to inhibit parasite DNA topoisomerase II activity *in vitro* for malaria study (Auparakkitanon & Wilairat, 2000).

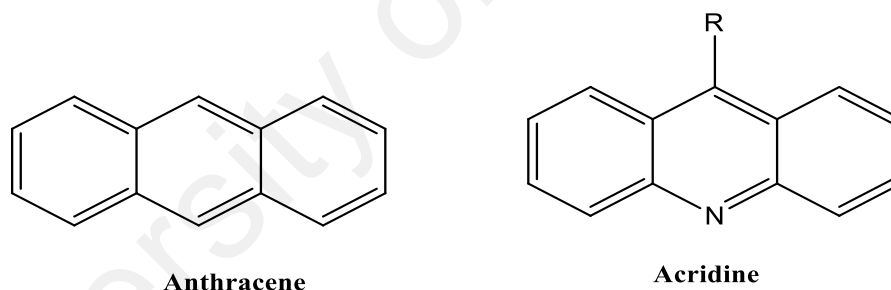


**Figure 2.1:** The similarity skeleton of acridine and anthracene

Acridine was derived from the synthesis pathways, which has similarity as xanthone (Ba-gen et al., 2014; Goodell et al., 2006; See et al., 2014) as shown in **Figure 2.2**. Xanthone was derived from the natural product of  $\alpha$ -mangostin that was isolated from various parts of the mangosteen *Garcinia mangostana L. (Clusiaceae)*. Aza-aromatic system consists in these parent structure allowed acridine or xanthone being evaluated as

anti-cancer agents (Yang et al., 2014) *via* cytotoxicity activity screening using human cancer cell lines (Giri et al., 2010)

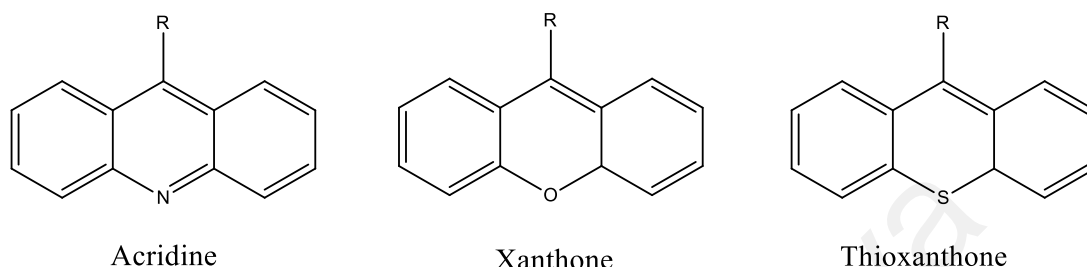


**Figure 2.2:** The skeleton of acridine, xanthone and thioxanthone

The parent acridine can exist in two tautomeric form – imine or amine form as shown in **Figure 2.3**. When the nitrogen atom binds to C-9 in acridine compound these two tautomeric will form. However the presence of the substituent will affect the equilibrium of tautomeric (Kumar et al., 2013; Mignon et al., 2013). Somehow different types of solvent might also change the two tautomers. Next, the delocalization of the  $\pi$ - $\pi$  electrons in the aromatic ring would enhance the tendency of acridine to bind with other substituents and the formation of organometallic or coordination compounds when reacted with metals (Kumar et al., 2016). The combination of acridine molecule with metals will improve the potential and behavior of acridine derivatives. Heavy metals such as platinum, palladium and gold are used to bind with ligand or organic compound (Becka et al., 2017; Prajina et al., 2016; Zhao et al., 2015). An example of 1-acridin-9-yl-3-methylthiourea Au(I) is a complex that displays its antiproliferative activities specially by interfering with mitochondrial thioredoxin reductase (TrxR) (Pereira et al., 2017; Perez et al., 2017). In addition, acridine derivatives have been identified to trigger their antitumor properties through the inhibition of different enzyme. Acridine derivatives

form a ternary complex in which it is intercalated into DNA and the aniline side chain interacts with the enzyme in biological application (Kumar et al., 2017).

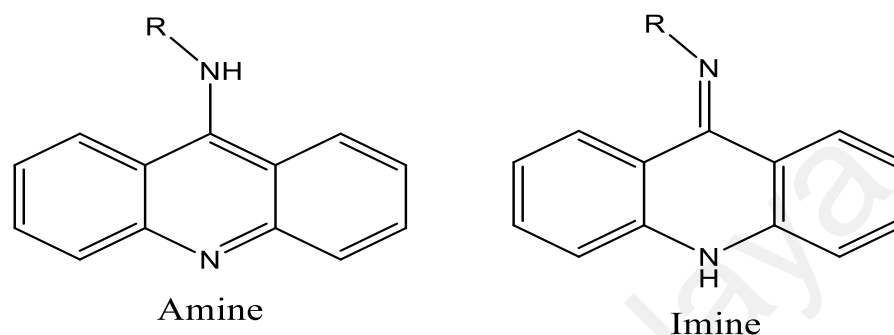


**Figure 2.3:** Two tautomeric form of 9-aminoaniline

## 2.2 Platinum complexes

Platinum is group VIII in periodic table of the transition metals which is the heaviest member compared to other metal. The cisplatin is one example compound from this group having potential uses in the cure of several diseases (Lovejoy & Lippard, 2009). Metal-based drugs have been known since very ancient time's either soft or heavy metals. For example soft metal, silver employed in the treatment of wounds and ulcers (Medici et al., 2015). In medicine, metal-based started almost 50 years when cisplatin was shown to inhibits cellular division which directly have attention of researchers because pool of transition "heavy" metals as potential therapeutic agents.

Besides that, the fact that platinum is much more inert than palladium, is not surprising that the preparation of cycloplatinated primary amines still remains uncommon and its general synthetic methods need to be further develop. Platinum complexes (Dell' Amico et al., 2015; Gallego et al., 2007; Sun et al., 2013; Zhao et al., 2014) which is square-

planar cyclometallated, currently studied for purposes which include the preparation of bio-active molecules in anticancer and the synthesis of new photo-active materials (Matesanz et al., 2014)

Other than that, palladium (II) (Aguirre et al., 2007; Matesanz et al., 2013) have their own behavior in term of chelating with ligands, which is differ from Pt(II). They expose a greater propensity to exchange their ligands. So, the rapid hydrolysis of palladium-based drugs can occur easily. Palladium complexes are inactive as therapeutically agent but toxic due to higher reactivity. Pd(II) complexes have been reported the cytotoxicity activity against human myelogenous leukemia and prostate cancer (Aguirre et al., 2007; Budzisz et al., 2007; Ramachandran et al., 2012).

Metals chelating with compounds containing N, S and O donor atoms show broad biological activity, because of the lone pair of that atoms will binds to the DNA or protein. Ligands containing these atoms also will enhance the cyclometallation with metals due to the variety of ways, they can coordinate to metal. Cyclometallation of N-donor ligands by platinum, palladium or other metals was remained as one of the major topics in organometallic chemistry (Guo et al., 2017). Although a large variety of N-containing ligands have been successfully cyclometalated, however its take long time to unfold the synthesis method.

### **2.3 The biological important of acridine and its derivatives**

In medicinal and pharmaceutical research, designing and development of anticancer drugs exhibiting superior cytotoxicity with strong DNA and protein binding ability are highly entreat, in order to expand and improve cancer therapy. One of a central role in cancer chemotherapy, widely used as platinum-based anticancer drug is cisplatin [*cis-*

diamminedichloroplatinum (II)]. Cisplatin currently endorse the treatment of testicular cancer ovarian and bladder (Chen et al., 2018; Comsa et al., 2018; Obrist et al., 2018). Proteins and phospholipids are the biomolecule which the reaction take place where cisplatin are induce in cancer cells. However, the drugs is rapidly distributed throughout the whole body upon administration, interacting both with healthy and cancerous tissues. There are a few effects cause by cisplatin which are nephrotoxicity, emetogenesis and neutotoxicity. In simple word, it could reverse the degeneration of normal cells which can cause cancer.

Starting from that issues, there are many researchers dig the knowledge of synthesizing or modifying of all anticancer drugs which may be lead to the discovery of new compounds that can contribute to the biomedical research (Chen et al., 2009; Gama et al., 2012; Temple et al., 2002). Acridine derivatives is one of the compound that shows good potential as anticancer especially when intercalating with DNA or RNA (Chang et al., 2003). There are two ways of interaction of DNA with nuclei acids of acridine derivatives, either (i) *via* intercalation between double-stranded DNA base pairs and inhibition of a DNA topoisomerase II Amsacrine enzyme or (ii) *via* stabilization of alternative four stranded DNA structures call G-quadruplexes, BRACO-19 (9-(4-(N,N-dimethylamino)phenylamino)-3,6-bis(3-pyrrolidinopropion amido) acridine) (Medapi et al., 2016; Olszewska et al., 2014). The acridine-based drug which is 9-aminoacridine hydrochloride hydrate showed better antibacterial efficacy when they conjugated with gold nanoparticle against strains of Gram positive and Gram negative bacteria (Mitra et al., 2014). The use of antibiotics and inorganic nanoparticle together is the best idea because bacteria have resistance against one of the components, while another component could kill them in a different manner. (Kim et al., 2017).

## CHAPTER 3: METHODOLOGY

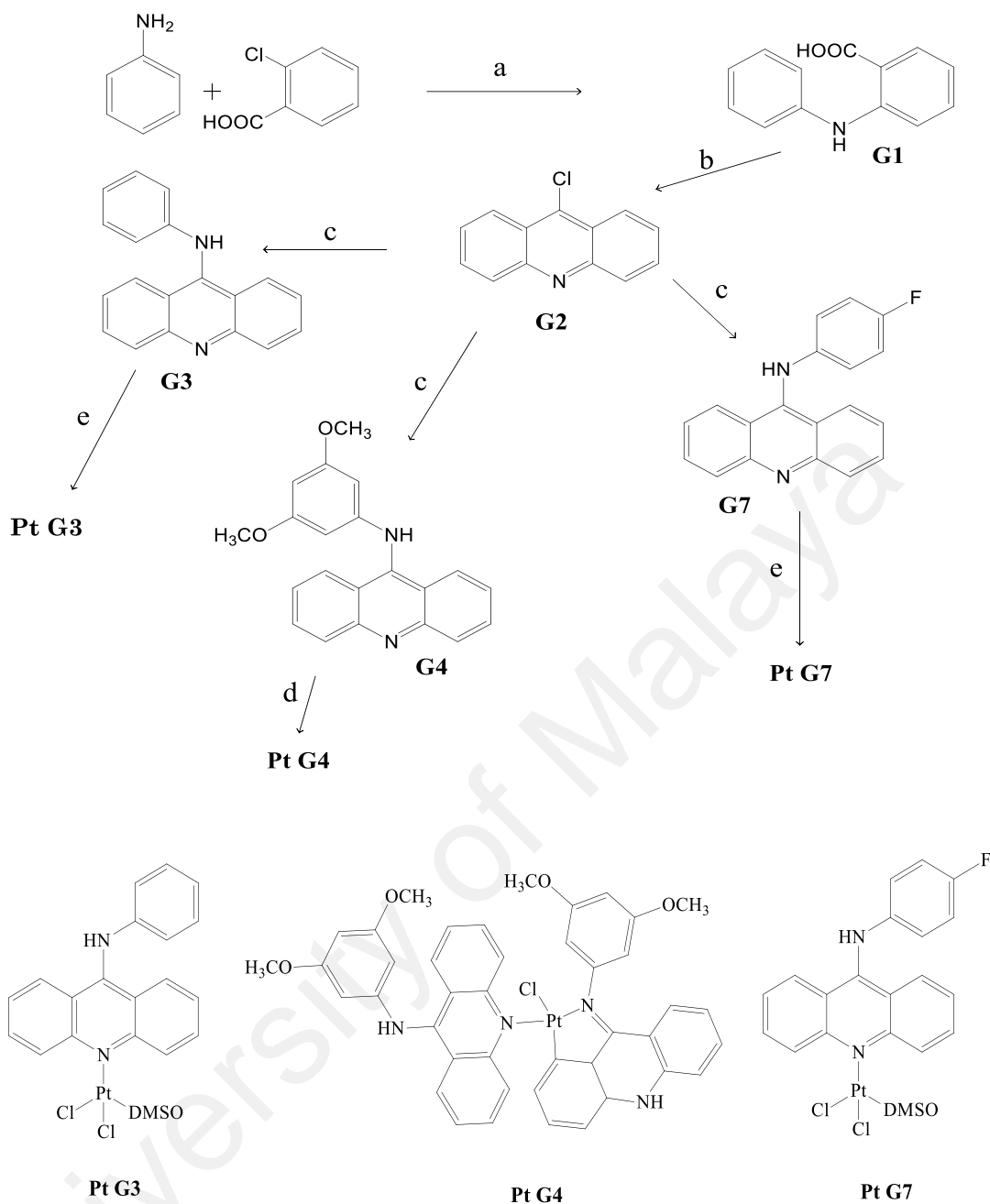
### 3.1 Materials and Instrumentation

The chemicals and solvents were obtained from Merck, Sigma Aldrich or Fisher Scientific and used without further purification unless stated otherwise. The 2-(phenylamino)benzoic acid was synthesized according to the described procedure (Lang et al., 2013; Li et al., 2014) with slight modifications.

The Infrared (IR) spectra of the synthesized compounds were recorded using Perkin Elmer FTIR spectrometer within the range of 400-4000  $\text{cm}^{-1}$ . The Nuclear Magnetic Resonance of protons ( $^1\text{H}$  NMR) and carbons ( $^{13}\text{C}$  NMR) spectra were recorded on AVN Bruker 400 FT-NMR and Jeol ECX DELTA 400 MHz spectrometer using deuterated DMSO or chloroform as solvent. Elemental analyses for the determination of the carbon, hydrogen and nitrogen (CHN) compositions were performed by using elemental analyzer Perkin Elmer CHNS/O 2400 series II. Thermal gravimetric analysis was recorded on a Perkin Elmer TGA 4000 thermogravimetric analysis (TGA). The single crystal X-ray diffraction data collection of some of the complexes were performed on a Bruker APEX II CCD diffractometer at 100 K employing graphite-monochromated Mo  $K\alpha$  radiation ( $\lambda=0.71073\text{\AA}$ ). The intensities were collected using  $\omega - 2\theta$  scan mode in the range of  $3.1^\circ < \theta < 26.0^\circ$ . All structures were solved using a direct method by SHELXS-97 program (Sheldrick, 2008) and refined by a full matrix least-square method on  $F^2$  using SHELXL-97 program package (semi-empirical absorption corrections were applied using SADABS program). The melting points of the compounds were determined using a capillary melting point apparatus, MEL-TEMP II Laboratory Devices USA.

### 3.2 General preparation of ligands and their complexes

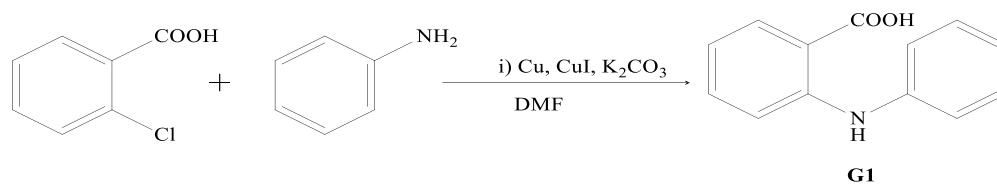
The routes towards synthesizing the acridine derivatives involve four steps as shown in **Scheme 3.1**. First part is to bind the aniline with 2-chlorobenzoic acid to form the 2-(phenylamino)benzoic acid, **G1** which consists of secondary amine group. Next, the cyclization of, **G1** occur when react with phosphorous oxychloride ( $\text{POCl}_3$ ) at 135 °C overnight, (Kalirajan et al., 2012) the yellow precipitate of 9-chloroacridine, **G2** formed. Then, **G2** react with aniline to form acridin-9-ly-phenyl-amine **G3**, acridin-9-ly-(3,5-dimethoxy-phenyl)-amine **G4** and acridin-9-ly-(4-fluoro-phenyl)-amine **G7**. Two methods were utilized to synthesis the Pt complexes. The **Pt G3** and **Pt G7** was reacted with *cis*-dichloro(dimethylsulfoxide) (*cis*- $\text{PtCl}_2(\text{DMSO})_2$ ) in absolute ethanol as solvent and sodium acetate (NaOAc) as base. The **Pt G4** however, was reacted with Pt using mixture of methanol:toluene (2:1) as solvent.



**Scheme 3.1:** General overview to produce derivatives of acridine. Reagents and conditions: (a)  $\text{K}_2\text{CO}_3$ , Cu, CuI, DMF, 130 °C; (b)  $\text{POCl}_3$ , 138 °C, (c)  $\text{K}_2\text{CO}_3$ , KI, absolute ethanol, 78 °C; (d)  $\text{PtCl}_2\text{DMSO}_2$ , NaOAc, methanol:toluene (2:1), 65 °C; (e)  $\text{PtCl}_2\text{DMSO}_2$ , NaOAc, ethanol

### 3.3 Preparation of the precursors

#### 3.3.1 Synthesis of 2-(phenylamino)benzoic acid, G1

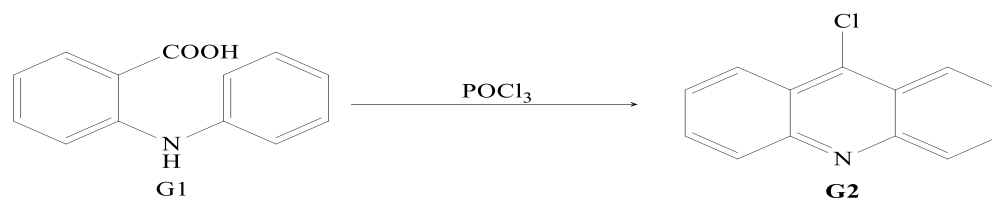


**Scheme 3.2:** Synthesis of 2-(phenylamino)benzoic acid, G1

A **G1** was synthesized using a similar procedure as previously described (Lang et al., 2013; Li et al., 2014). 2-chlorobenzoic acid (6.0 g, 38.32 mmol), aniline (4.28 g, 45.98 mmol), potassium carbonate required to remove excess of chlorine in reaction, (10.59 g, 76.64 mmol), copper powder (1.22 g, 19.16 mmol) and copper iodide (1.83 g, 9.58 mmol) was dissolved in DMF and refluxed at 130 °C in oil bath overnight. The copper act as catalyst to increase the reactivity of aryl amine to form **G1**. The reaction was followed by thin layer chromatography (TLC). The reaction mixture was cooled to room temperature after the reaction completed. Then, 30 mL of water was poured into the reaction mixture that was first added with decolorized charcoal. The charcoal was used to remove or clean decant of undesired liquid from the precipitate. The mixture was filtered through celite. The crude product was obtained by precipitation upon acidification of the filtrate with dilute HCl (pH was adjusted 1 to 2). The solid residue was dissolved in 100 mL of 5% aqueous Na<sub>2</sub>CO<sub>3</sub>. Then, the filtration through celite was repeated to obtain the final product, 2-(phenylamino)benzoic acid **G1** (**Scheme 3.2**). Yield: (4.4 g; 54.3%); mp (148.0-150.0 °C) Anal. Calc. for C<sub>13</sub> H<sub>11</sub> N O<sub>2</sub> (213.1): C, 72.54; H, 6.09; N, 6.5. Found: C, 71.96; H, 5.98; N, 6.87. IR (cm<sup>-1</sup>): 3333.4 ν (N-H), 3026.0 ν (O-H), 1657.0 ν (C=O), 1262.3 ν (C-N); <sup>1</sup>H-NMR (400MHz, CDCl<sub>3</sub>) 9.24 (s, 1H, N-H), 7.97 (dd, *J* = 8.0 Hz; 1H, Ar-H), 7.30 (m, 3H, Ar-H), 6.76 (m, 1H, Ar-H), 6.38 (t, *J* = 8.0 Hz; 3H, Ar-H), 6.19 (d, *J* = 8.0 Hz; 1H, Ar-H); <sup>13</sup>C-NMR (100MHz, CDCl<sub>3</sub>, ppm) 173.26 (C=O), 148.92 (C-

C=O), 140.36 (C-NH), 135.19, 132.61, 129.44, 124.10, 123.15, 117.19 and 114.04 (C-Ar).

### 3.3.2 Synthesis of 9-chloroacridine, G2

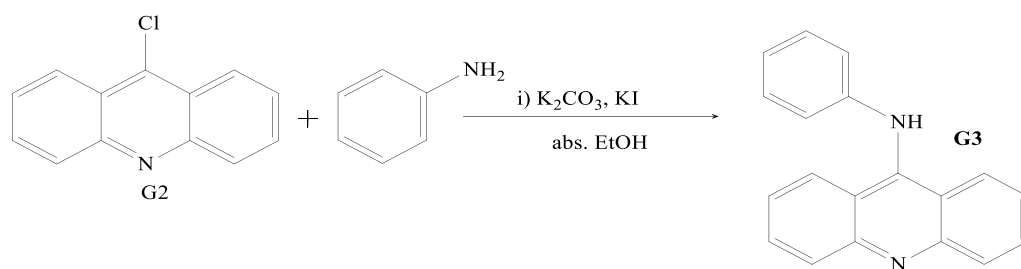


**Scheme 3.3:** Synthesis of 9-chloroacridine, G2

A mixture of 2-(phenylamino)benzoic acid **G1** (4.0 g, 18.76 mmol) and POCl<sub>3</sub> (39.40 g, 256.71 mmol) was heated slowly in oil bath at 85-90 °C for 15 min. The temperature was increased to 135-140 °C and maintained under reflux for 3 hr. Upon the completion of the reaction, an excess of phosphorous oxychloride was removed by vacuum distillation. After cooling to room temperature, the reaction mixture was poured into a well-stirred mixture of 25 mL concentrated ammonia and crushed ice, then allowed to stand for 30 min for product precipitation. The precipitate was filtered by suction, washed three times with 20-50 mL of 5% of NaHCO<sub>3</sub> and finally with water. The precipitate of 9-chloroacridine **G2** (**Scheme 3.3**) was dried over phosphorus pentoxide and recrystallization from ethanol form a pale brown crystal. Yield: (2.4 g, 60.0%); mp (118.0-120.0 °C). Anal. Calc. for C<sub>13</sub> H<sub>8</sub> N Cl (213.7): C, 73.08; H, 3.77; N, 6.56; Cl, 16.59. Found: C, 72.96; H, 4.26; N, 6.79. IR (cm<sup>-1</sup>): 3050.0 (C-HAr), 1631.8 (C=N), 1542.0 (C=C), 747.8 (C-Cl) cm<sup>-1</sup>; <sup>1</sup>H-NMR (400 MHz, CDCl<sub>3</sub>) 8.37 (d, 2H, 3J=8.7 Hz, H-4, H-5), 8.17 (d, 2H, 3J= 8.8 Hz, H-1, H-8), 7.74 (ddd, 2H, 3J = 6.6 Hz, H-3, H-6), 7.56 (ddd, 2H, 3J= 6.7 Hz, H-2, H-7). <sup>13</sup>C NMR (100 MHz, CDCl<sub>3</sub>): 149.0 (C-Cl) 141.17 (C-N), 130.57, 129.83, 126.93, 124.66, 124.32 (C-N).

### 3.4 Preparation of ligands and Platinum complexes

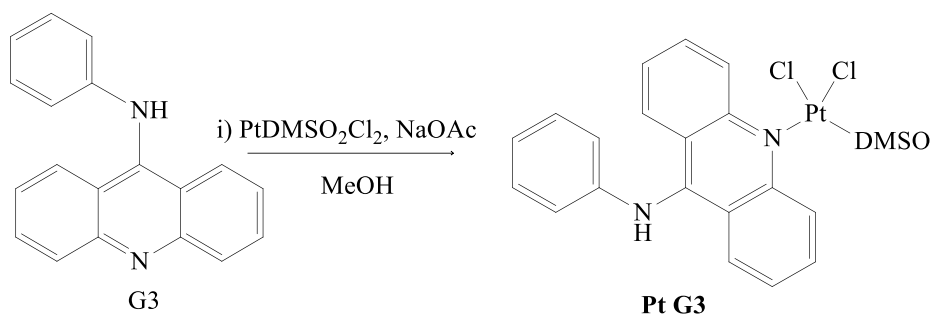
#### 3.4.1 Synthesis of N-phenylacridin-9-amine, G3



**Scheme 3.4:** Synthesis of N-phenylacridin-9-amine, G3

A **G2** (1.0 g, 4.68 mmol) was dissolved in 50 mL absolute ethanol. To this mixture, aniline (0.87 g, 9.36 mmol) was added followed by K<sub>2</sub>CO<sub>3</sub> (1.29 g, 9.36 mmol) and KI (0.2 g, 1.17 mmol). The reaction mixture was heated under reflux for 18.0 hr. The TLC showed no leftover of the starting materials; hence the solvent was evaporated to dryness to proceed with a separation method. The remaining mixture was extracted with dichloromethane against water. The organic layer was dried over magnesium sulphate then concentrated. The product was obtained as yellow precipitate and washed with cold methanol. The crude product *N*-phenylacridin-9-amine **G3** (**Scheme 3.4**) was recrystallized from ethanol to purify it. Yellow crystalline materials were obtained after few days. Yield (1.0 g, 76.0%) mp. (294.0-296.0 °C) Anal. Calc. for C<sub>19</sub>H<sub>14</sub>N<sub>2</sub> (207.3): C, 84.42; H, 5.22; N, 10.36, Found: C, 84.41; H, 4.42; N, 10.42. IR (cm<sup>-1</sup>): 3358.1 (N-H), 1614.3 (C=N), 1583.5 (C=C), 1326.2 (C-N) cm<sup>-1</sup>. <sup>1</sup>H NMR (400 MHz, CDCl<sub>3</sub>) δ: 11.03 (s, 1H, NH), 8.10 (d, 2H, <sup>3</sup>J = 8.4 Hz, H-4, H-5), 8.01 (d, 2H, <sup>3</sup>J = 9.0 Hz, H-1, H-8), 7.51 (dd~d, 2H, <sup>3</sup>J = 8.0 Hz, Ar-H), 7.42 (dd~d, 1H, Ar-H), 7.39 (d, 2H, <sup>3</sup>J = 8.0 Hz, Ar-H), 7.37 (dd~d, 1H, <sup>3</sup>J = 7.0 Hz, Ar-H), 7.29 (t, 1H, <sup>3</sup>J = 7.5 Hz, Ar-H), 7.00 (b-dd, 2H, <sup>3</sup>J = 7.0 Hz, Ar-H). <sup>13</sup>C NMR (100 MHz, CDCl<sub>3</sub>): 154.06 (C-NH), 141.38 (C-N), 139.71, 134.51, 130.16, 127.13, 126.13, 123.99 C, 123.38, 119.89, 114.91 (C-Ar).

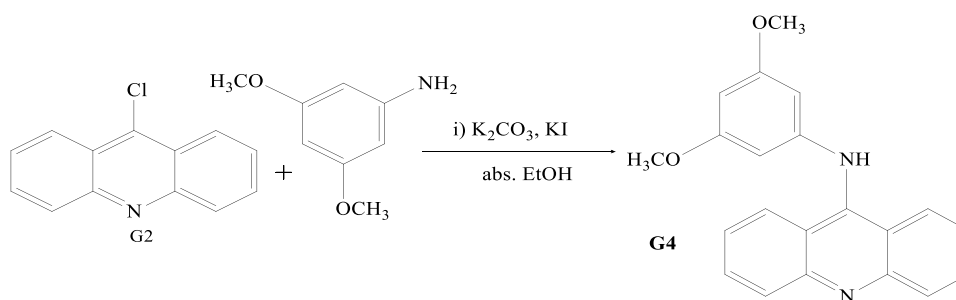
### 3.4.2 Synthesis of (N-phenylacridin-9-amine)cis-dichloro(dimethylsulfoxide)-platinum(II), Pt G3



**Scheme 3.5:** Synthesis of (N-phenylacridin-9-amine)cis-dichloro(dimethylsulfoxide)-platinum(II), Pt G3

A **G3** (0.2 g, 0.7 mmol) was dissolved in 20.0 mL methanol, followed by sodium acetate (0.1 g, 0.7 mmol) and *cis*-[PtCl<sub>2</sub>(DMSO)<sub>2</sub>] (0.3 g, 0.7 mmol). The mixture was heated to reflux for 4 days in oil bath and monitored by TLC to confirm the reaction completion. A brownish-orange precipitate (N-phenylacridin-9-amine)cis-dichloro(dimethylsulfoxide)-platinum(II) **Pt G3** (Scheme 3.5) was formed during the reaction, which was then filtered out and dried over phosphorus pentoxide. Yield: (0.2 g, 51.0%); m.p. (260.0-262.0 °C). Anal. Calc. for C<sub>21</sub>H<sub>20</sub>Cl<sub>2</sub>N<sub>2</sub>OPtS (614.45): C, 41.05; H, 3.28; N, 4.56; S, 5.33; Found: C, 38.98; H, 2.65; N, 4.34. IR (cm<sup>-1</sup>): 3321 (N-H), 3040 (C-H<sub>Ar</sub>), 1612 (C=N), 1568, (C=C), 1267 (C-N), 1020 (S=O) cm<sup>-1</sup>. <sup>1</sup>H NMR (400 MHz, DMSO-*d*<sub>6</sub>) 10.20 (s, 1H, NH), 9.83 (d, 2H, <sup>3</sup>J = 8.5 Hz, H-4, H-5), 8.17 (dd~d, 2H, <sup>3</sup>J = 8.4 Hz, H-1, H-8), 8.03 (ddd, 2H, <sup>3</sup>J = 8.0 Hz, Ar-H), 7.43 (ddd, 2H, <sup>3</sup>J = 7.0 Hz, Ar-H), 7.32 (dd, 2H, <sup>3</sup>J = 7.5 Hz, Ar-H), 7.12 (b-t, 1H, <sup>3</sup>J = 7.5 Hz, Ar-H), 7.37 (dd~d, 1H, <sup>3</sup>J = 7.0 Hz, Ar-H), 7.29 (t, 1H, <sup>3</sup>J = 7.5 Hz, Ar-H), 7.00 (b-ddd, 2H, Ar-H), 7.08-7.02 (m<sub>c</sub>, 2H, Ar-H), 3.35 (s, 6H, 2x CH<sub>3</sub>). <sup>13</sup>C NMR (100 MHz, DMSO-*d*<sub>6</sub>): 150.35 (C-4a, C-5a), 148.02 (C-9), 143.57 (C-12), 133.20 C-Ar, 132.34 C-Ar, 129.66 C-Ar, 128.12 C-Ar, 124.98 (C-1, C-8), 124.21 C-Ar, 121.14 (C-4, C-5), 118.45 (C-8a, C-9a), 40.43 (S-CH<sub>3</sub>).

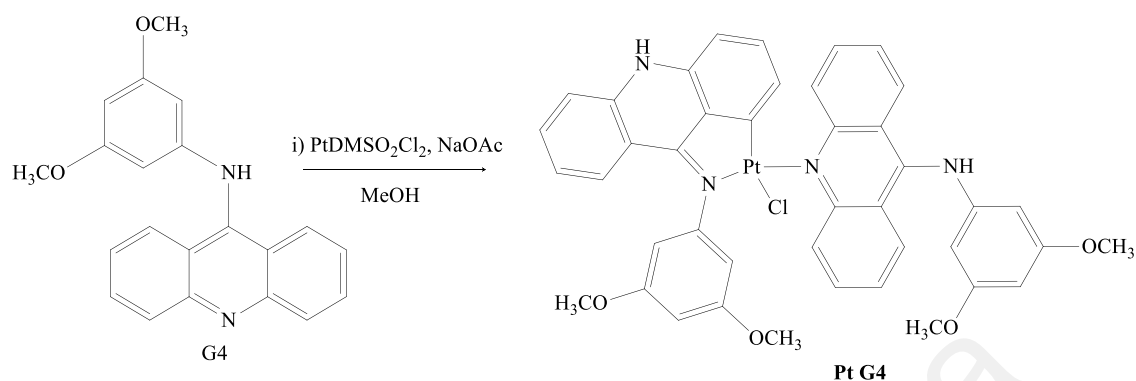
### 3.4.3 Synthesis of N-(3,5-dimethoxyphenyl)acridin-9-amine, G4



**Scheme 3.6:** Synthesis of N-(3,5-dimethoxyphenyl)acridin-9-amine, G4

The 3, 5-dimethoxyaniline (0.7 g, 4.7 mmol) and potassium carbonate (0.7 g, 4.7 mmol) were dissolved in an absolute ethanol (15.0-20.0 mL). The mixture was stirred for 45 min at room temperature, then a **G2** (0.5 g, 2.3 mmol) and potassium iodide (0.1 g, 0.6 mmol) were added. The mixture was further stirred and refluxed overnight. Upon the reaction completion the solvent was evaporated, and the solid obtained was poured into a 50.0 mL water and extracted with ethyl acetate to give a crude product. The orange precipitate of *N*-(3,5-dimethoxyphenyl)acridin-9-amine, **G4** (**Scheme 3.6**) was filtered and washed with a cold methanol then dried. Yield: (0.7 g, 91.8%); mp (184.0-186.0 °C); Anal. Calc. for C<sub>21</sub> H<sub>18</sub> N<sub>2</sub> O<sub>2</sub> (330.4): C, 76.34; H, 5.49; N, 8.48. Found: C, 75.96; H, 5.26; N, 10.79. IR (cm<sup>-1</sup>): 3358.7 ν (N-H), 1614.2 ν (C=N), 1581.8 ν (C-C), 1170.3 ν (C-O); <sup>1</sup>H-NMR (400 MHz, CDCl<sub>3</sub>/TMS, ppm) 8.26 (d, *J* = 8 Hz; 2H, Ar-H), 8.16 (d, *J* = 8 Hz; 2H, Ar-H), 7.45 (t, *J* = 8 Hz; 2H, Ar-H), 7.09 (t, *J* = 8 Hz; 2H, Ar-H) 6.56 (d, *J* = 4 Hz; 2H, Ar-H), 6.23 (t, *J* = 4 Hz; 1H, Ar-H), 3.64 (s, 6H, OCH<sub>3</sub>); <sup>13</sup>C-NMR (100 MHz, CDCl<sub>3</sub>) 161.62 (C-O-CH<sub>3</sub>), 154.32, 142.81 (C-N), 139.95, 134.49, 126.32, 123.91, 119.76, 114.78, 101.91, 99.07 (C-Ar) and 55.61 (O-CH<sub>3</sub>).

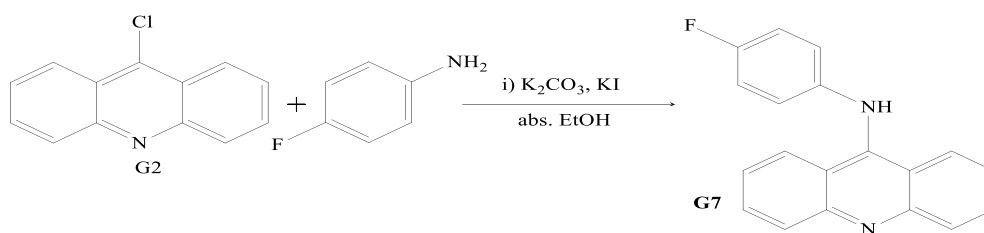
### 3.4.4 Synthesis of (N-(3,5-dimethoxyphenyl)acridin-9-amine) cis-dichloro (dimethylsulfoxide) platinum(II), Pt G4



**Scheme 3.7:** Synthesis of (N-(3,5-dimethoxyphenyl) acridin-9-amine) cis-dichloro(dimethylsulfoxide) platinum(II), Pt G4

A **G4** (0.5 g, 1.5 mmol) was dissolved in 20.0 mL of a mixture of toluene:methanol (1:1), separately dissolved sodium acetate (0.1 g, 1.5 mmol) and *cis*-[PtCl<sub>2</sub>(DMSO)<sub>2</sub>] (0.6 g, 1.5 mmol) in the solvent mixture, then added to the **G4** solution. The mixture was heated to reflux for 4 days in oil bath and monitored by TLC to confirm the reaction completion. A brownish-orange precipitate of (N-(3,5-dimethoxyphenyl)acridin-9-amine)*cis*-dichloro(dimethylsulfoxide)-platinum(II), **Pt G4** (Scheme 3.7) was formed during the reaction, which was then filtered out and dried over phosphorus pentoxide. Yield: (0.7 g, 53.1%); mp (224.0-226.0 °C); Anal. Calc. for C<sub>42</sub> H<sub>35</sub> Cl<sub>2</sub> N<sub>4</sub> O<sub>4</sub> Pt (890.3): C, 51.91; H, 4.38; N, 5.75. Found: C, 40.80; H, 3.69; N, 4.42. IR (cm<sup>-1</sup>): 3322.4 ν (N-H), 2921.1 ν aromatic, 1468.3 ν (C=N), 1488.7 ν (C=C), 1125.1 ν (C-O), 761.69 ν (C-Cl), 488.6 ν (C-Pt); <sup>1</sup>H-NMR (400 MHz, DMSO- *d*<sub>6</sub> TMS, ppm) 10.11 (d, *J* = 8 Hz; 2H, Ar-H), 9.82 (d, *J* = 8 Hz; 1H, N-H), 9.72 (d, *J* = 8 Hz; 2H, Ar-H), 8.20 (m, 4H, Ar-H) 8.00 (m, 4H, Ar-H), 7.48 (m, 4H, Ar-H), 6.27 (d, *J* = 8 Hz; 2H, Ar-H), 6.19 (d, *J* = 8 Hz; 2H, Ar-H), 6.14 (d, *J* = 8 Hz; 1H, Ar-H), 3.62 (s, 6H, OCH<sub>3</sub>) and 3.49 (s, 6H, OCH<sub>3</sub>); <sup>13</sup>C-NMR (100MHz, DMSO- *d*<sub>6</sub>) 161.64 (C-O-CH<sub>3</sub>), 141.42, 134.01 (C-N), 150.48, 148.09 145.91, 132.84, 128.42, 126.55, 125.38, 124.57, 121.55, 119.16, 117.87, 99.07, 96.31 (C-Ar) and 55.78 (O-CH<sub>3</sub>).

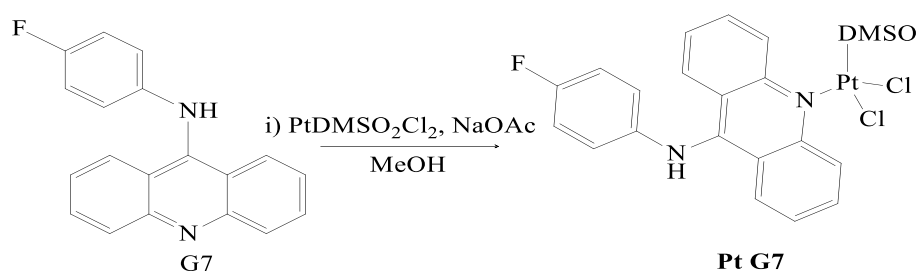
### 3.4.5 Synthesis of N-(4-fluorophenyl)acridin-9-amine, G7



**Scheme 3.8:** Synthesis of N-(4-fluorophenyl)acridin-9-amine, G7

A **G2** (1.0 g, 4.7 mmol) was added to a round bottomed flask with potassium iodide (3.1 g, 18.7 mmol) and dissolve in absolute ethanol 20.0 mL. Then a 4-Fluoroaniline (10.4 g, 9.4 mmol) and potassium carbonate (1.3 g, 9.4 mmol) were added. The reaction was stirred and refluxed for 18.0 hr. The mixture was extracted with water (50.0 mL) and ethyl acetate. The precipitate of N-(4-fluorophenyl)acridin-9-amine **G7** (**Scheme 3.8**) was then filtered off by cold methanol and dried over silica-gel. Yield: (0.2 g, 58.1%); mp (162.0-164.0 °C); Anal. Calc. for C<sub>19</sub>H<sub>13</sub>FN<sub>2</sub> (288.3): C, 79.15; H, 4.54; F, 6.59; N, 9.72. Found: C, 79.33; H, 4.88; N, 9.34. IR (cm<sup>-1</sup>): 3460.5 v (N-H), 1628.2 v (C=N), 1505.7 v (C=C), 1219.5 v (C-F); <sup>1</sup>H-NMR (400 MHz, DMSO-*d*<sub>6</sub>) 11.23 (s, 1H, N-H), 7.82 (s, 2H, Ar-H), 7.50 (dt, J = 8 Hz; 4H, Ar-H), 7.12 (dt, J = 8 Hz; 2H, Ar-H) 7.00 (t, J = 2 Hz; 2H, Ar-H), 6.82 (dt, J = 4 Hz; 2H, Ar-H); <sup>13</sup>C-NMR (100 MHz, DMSO-*d*<sub>6</sub>) 160.39 (C-F), 158.03, 152.96, 141.41, 117.88 (C-N), 133.30, 126.96, 122.73, 122.26, 119.25, 117.88, 117.05 and 116.83 (C-Ar).

**3.4.6 Synthesis of (N-(4-fluorophenyl) acridin-9-amine) cis-dichloro (dimethylsulfoxide) platinum(II) acridine, Pt G7**



**Scheme 3.9:** Synthesis (N-(4-fluorophenyl) acridin-9-amine) cis-dichloro (dimethylsulfoxide) platinum(II) acridine, Pt G7

A **G7** (0.2 g, 0.7 mmol) was dissolved in 20.0 mL methanol, followed by sodium acetate (0.06 g, 0.7 mmol) and *cis*-[PtCl<sub>2</sub>(DMSO)<sub>2</sub>] (0.29 g, 0.7 mmol). The mixture was heated to reflux for 4 days in oil bath and monitored by TLC to confirm the reaction completion. A solid precipitate of (N-(4-fluorophenyl)acridin-9-amine)*cis*-dichloro(dimethylsulfoxide)-platinum(II) acridine, **Pt G7** (**Scheme 3.9**) was formed during the reaction, which was then filtered out and dried over phosphorus pentoxide. Yield: (0.3 g, 62.1%); mp (240.0-242.0 °C); Anal. Calc. for C<sub>21</sub> H<sub>18</sub> Cl<sub>2</sub> F N<sub>2</sub> Pt S (631.4): C, 41.98; H, 2.87; F, 3.01; N, 4.44. Found: C, 41.91; H, 3.36; N, 4.44. IR (cm<sup>-1</sup>): 3325.1 ν (N-H), 3003.0 ν (C-H<sub>Ar</sub>), 1567.9 ν (C=N), 1450.71 ν (C=C), 1140.8 ν (C-F), 756.0 ν (C-Cl), 490.3 ν (C-Pt); <sup>1</sup>H-NMR (400 MHz, DMSO-*d*<sub>6</sub>) 10.18 (s, br, 1H, N-H), 9.80 (dd, 2H, Ar-H), 8.15 (d, *J* = 8 Hz; 2H, Ar-H), 8.00 (m, 2H, Ar-H) 7.44 (td, *J* = 2 Hz; 2H, Ar-H), 7.15 (m, 4H, Ar-H); <sup>13</sup>C-NMR (100 MHz, DMSO-*d*<sub>6</sub>) 191.83, 189.58 (C-F), 183.94 168.80, 168.04, 132.73 (C-N), 133.59, 128.60, 125.33, 124.63, 123.94, 123.86, 117, 116.77 (C-Ar) and 44.45 (S-CH<sub>3</sub>).

### **3.5 Biological activity**

The biological activities cytotoxicity and acute toxicity were done at the Department of Pharmacy, Faculty of Medicine, University of Malaya 50603 Kuala Lumpur. The cytotoxicity testing was done by Dr Landa Zeebelabdin Ali using all of the synthesized compounds where acute toxicity test was done only for selected compound which was **G4**, done by Dr Mohamad Yousif Ibrahim. The detail experimental procedures are as follows.

#### **3.5.1 In vitro cytotoxicity Assay**

Cell cultures were maintained in humidified air with 5% CO<sub>2</sub> at 37 °C. MTT assay is currently the most commonly-used method to test the cytotoxicity of acridine and its metal complexes. The cells were plated in triplicates on a 96-well plate at a density of  $2 \times 10^5$  cells/mL in 100 µL of culture medium. Different concentrations of all compounds (50, 25, 12.5, 6, 3, and 1.5 µg/mL) were prepared by serial dilution. All serial dilutions were transferred to the cells in the 96-well plates. Untreated cells acted as the control. The cells were incubated for 24 hours, after which their viability was assessed by adding 20 µL of 3-(4,5-dimethylthiazol-2-yl)-2,5-diphenyltetrazolium bromide (MTT, 5 mg/mL) to the cells in a dark room. The cells were then covered with aluminium foil and incubated for another 4 hours. Then, all the media were removed and 100 µL of DMSO added to the cells to solubilize the formazan crystals. Subsequently, the absorbance was read at a wavelength of 570 nm using a microplate reader. The test agents' cell growth inhibition abilities were expressed in terms of IC<sub>50</sub> (i.e. the concentrations at which cell growths were reduced by half).

### **3.5.2 Acute Toxicity Test for G4**

The acute toxicity study was carried out to determine a non-toxic dosage for **G4**. The protocol for this experiment was permitted by the ethics committee for animal experimentation of the Faculty of Medicine, University of Malaya. The animal were treated according to the National Academy of Science's Guide for the care and Use of Laboratory Animal.

### **3.6 Animal**

Mice of both genders were obtained from the Animal House Unit, Faculty of Medicine, University of Malaya (UM). All procedures on these animals were carried out in compliance with the regulations designated by the Institutional Animal Care and Use Committee, Faculty of Medicine, UM. The mice were kept in sterilized plastic cages with homogenized wood shavings as bedding. The ambient temperature was maintained at  $22 \pm 2$  °C, with 12 hours each of in the light-dark cycle and a relative humidity of 50 – 60%. Food and water were supplied at all times.

### **3.7 Experimental Animals**

Thirty-six mice (18 male and 18 female) were divided into three groups which were labelled as (1) group 1 or vehicle, which was administered 0.5% carboxymethyl cellulose (CMC) at 5 mL/kg; (2) group 2, which was administered 5 mL/kg of **G4** at 500 mg/kg; and (3) group 3, which was administered 5 mL/kg of **G4** at 1000 mg/kg. The animals were deprived of food overnight prior to treatment and for 3 – 4 hours after treatment. The purpose of the fasting was to eliminate all the food inside their gastrointestinal tracts that may otherwise complicate the absorption of the tested substance. The mice were

monitored for the development of toxicity signs within 48 hours after the intragastrical administration of **G4**. The number of deaths was recorded over 14 consecutive days. On the 15th day, all the mice were killed via xylazine-ketamine aesthetic overdose, following which histological (liver and kidney) evaluations and serum analyses were conducted according to the standard techniques (Ibrahim et al., 2010; Ibrahim et al., 2015).

### **3.8 Assessment of kidney and liver functions**

All biochemical assays were performed spectrophotometrically using a Hitachi-912 Autoanalyzer (Mannheim, Germany). Kidney functions were assessed in terms of anion gaps, blood urea nitrogen, as well as serum creatinine, sodium, potassium, chloride, and carbon dioxide levels. Serum alanine aminotransferase (ALT), alkaline phosphatase (ALP), gamma-glutamyl transferase (GGT), albumin, globulin, and bilirubin levels were also measured to evaluate the liver functions. All the serum samples were analysed in a blind manner to obtain data with good sensitivity and validity.

### **3.9 Assessment of lipid profile**

The concentrations of total cholesterol and high-density lipoprotein (HDL) cholesterol were estimated using the commercial kits by Span Diagnostics in accordance with the method described in the literature (Wybenga et al., 1970). The triglyceride concentrations were assessed by GPO-PAP end-point assay.

### **3.10 Histopathological examinations**

Renal and hepatic tissues were fixed in 10% formalin and embedded in paraffin, after which they were sectioned at intervals of 5  $\mu\text{m}$  and stained with hematoxylin-eosin solution. All sections were examined photomicroscopically (Olympus BH-2, Japan) by an independent histopathologist who had no knowledge of the treatment groups.

### **3.11 Measurement of lipid peroxidation**

The extent of lipid peroxidation was assessed with malondialdehyde (MDA) as the indicator. Initially, 10% (weight/volume) homogenates of kidney and liver specimens were obtained from 0.1 mol/L phosphate buffer which was centrifuged at 4 °C and 3500 rpm for 10 minutes. Then, 0.2 mL of supernatant was mixed with 0.67% 2-thiobarbituric acid (TBA) and 20% trichloroacetic acid solutions, followed by heating in a boiling water bath for 30 minutes. The absorbance of the pink chromogen formed by the reaction of TBA with MDA was measured at 532 nm. The results were expressed as MDA nmol/mg protein. The protein contents in the supernatant was measured via the Lowry method (Lowry et al., 1951).

### **3.12 Measurement of tissues glutathione**

Tissue samples were homogenized in 10 volumes of ice-cold 10% trichloroacetic and then centrifuged at 1000 rpm and 4 °C for 15 minutes. The supernatant was removed and re-centrifuged at 35000 rpm and 4 °C for 8 minutes. Glutathione (GSH) levels were determined using a spectrophotometric method, which is a modification of the Ellman procedure (Ellman, 1959).

### **3.13 Statistical analysis**

All data were expressed as means  $\pm$  SD and analysed using one-way ANOVA followed by post-hoc Tukey HSD multiple comparisons test. The type-1 error level was set  $P < 0.05$  for all tests. This entire process was performed using SPSS software (Chicago, IL, USA) version 19.0 for Microsoft Windows.

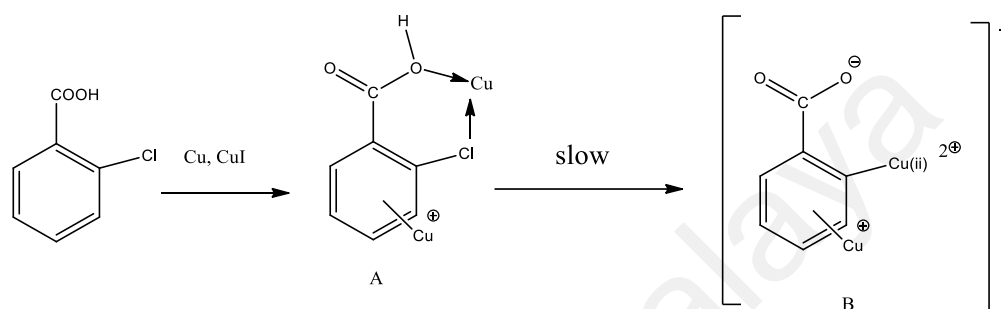
University of Malaya

## CHAPTER 4: RESULTS AND DISCUSSION

Three acridine derivatives with their Pt(II) complexes have been synthesized. All complexes were in different colours, depending on its ligands and it is soluble in dimethyl sulphoxide, but not in other common organic solvents. The acridine ligands however were soluble in chloroform. The structure of the compounds was established by using infrared (IR),  $^1\text{H}$  NMR and  $^{13}\text{C}$  NMR spectral data and were supported by the results of elemental analysis and X-ray Crystallography study. **Scheme 3.1** shows the general schematic diagram of the synthesis procedures. In general, four steps were involved, starting with the reaction of aniline with 2-chlorobenzoic acid. Then, the cyclization to form 9-chloroacridine, **G2** which further reacts with amine to form the ligands. The complexation reaction occur in a single step by reacting the ligand with Pt(II) salt. We report here the synthesis of **G3**, **G4** and **G7** ligands and **Pt G3**, **Pt G4** and **Pt G7** complexes. All compounds were subjected to biological activity testing, *in vitro* and *in vivo* to check its properties towards cancer cells and normal cells.

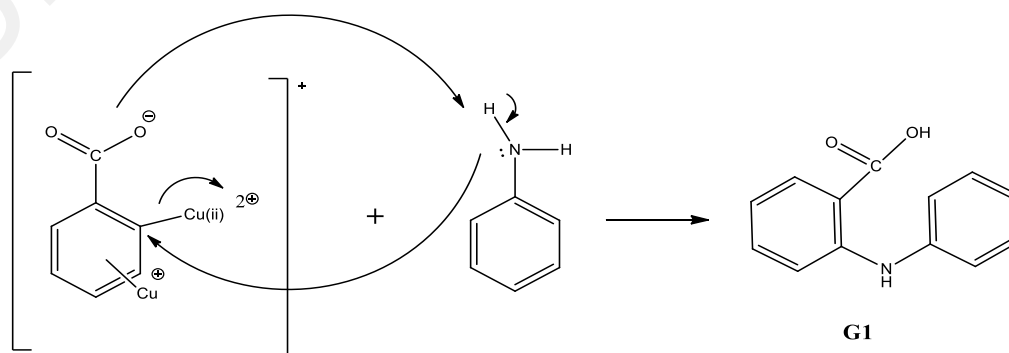
#### 4.1 Mechanism of action for synthesis of acridine derivatives and their complexes

There were three steps involved to produce the acridine derivatives. The first step utilized Ullmann reaction in which 2-chlorobenzoic acid and aniline were reflux in the presence of copper as catalyst. **Scheme 4.1** shows the mechanism of Ullmann reaction.



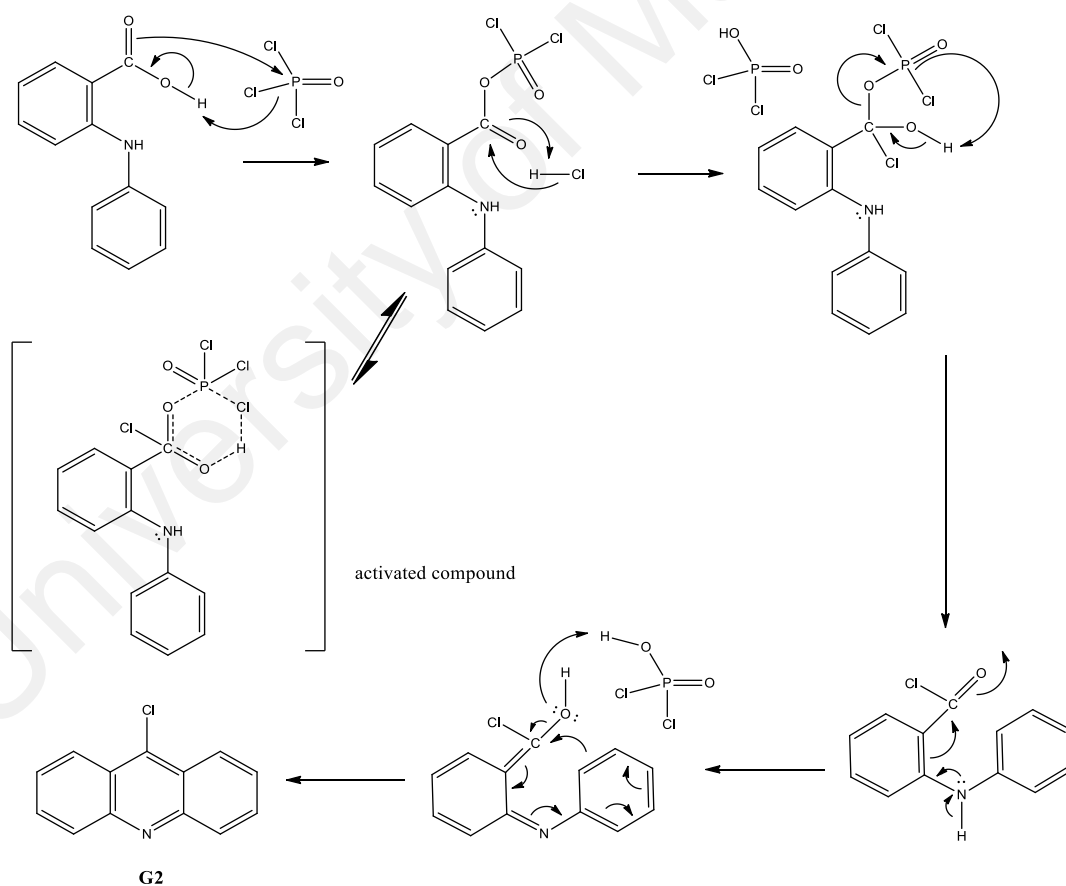
**Scheme 4.1:** Mechanism of Ullmann reaction

Structure A shows that lone pair from chlorine and oxygen in 2-chlorobenzoic acid, chelating with Cu metal, which increases the reactivity of the non-activated aryl amine towards aryl halide to afford the corresponding 2-phenylamino acid also known as N-phenylantranilic. The reaction was slow to form the intermediate B. This reaction was known as  $S_N2$  reaction. The transition state was fast then followed by the nucleophilic attack (aniline) to form the desired compound. **Scheme 4.2** shows the final step of forming 2-phenylamino acid, G1.



**Scheme 4.2:** Mechanism of 2-phenylamino benzoic acid, G1

Then, the preparation of 9-chloroacridine **G2**, involves cyclization of 2-phenylamino benzoic acid reacted with phosphoryl chloride in liquid without the use of any solvent to form acid chloride. The acid chloride was very reactive as compared to carboxylic acid. The electrophilic phosphorus atom was attacked by the nucleophile comes from oxygen of the carboxylic acid to form the activated compound (**Scheme 4.3**). HCl molecule react with the intermediate to form acid chloride. Next, the cyclization occur when lone pair of nitrogen attack the positive charged carbon atom. Second stage was the elimination of water, the hydroxyl group was pushed off, attacked by phosphoryl chloride ion and then promotes the delocalization of electrons from nitrogen atom and aromatic ring ended up with cyclization (Chandra et al., 2010; Perez et al., 2017)

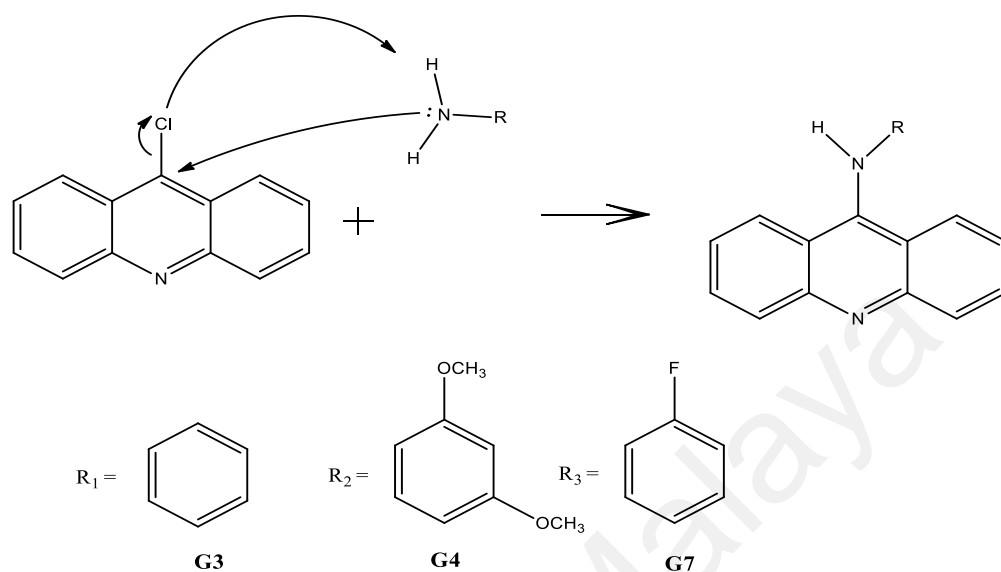


**Scheme 4.3:** Mechanism of cyclization to form 9-chloroacridine, **G2**

Various amines (**R**) were reacted with **G2** to form derivatives. The reaction starts with the nucleophilic attack of the positive carbon by the lone pair in of nitrogen atom. Then,

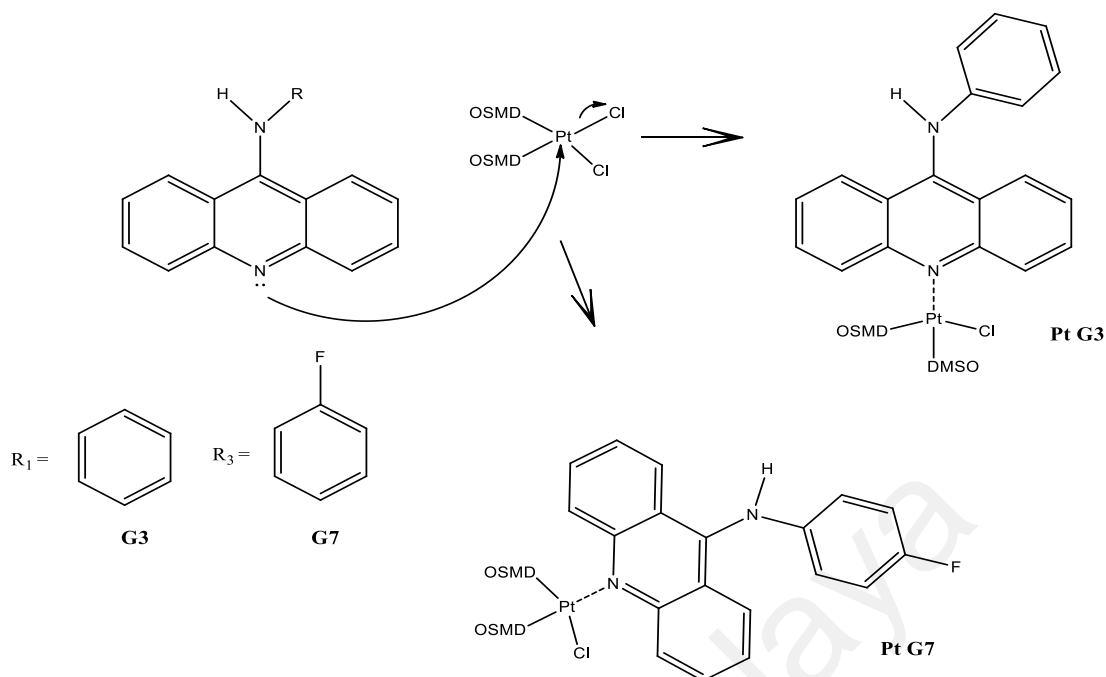
the second step was to remove the Cl<sup>-</sup> in the form of HCl that comes out as the by product.

**Scheme 4.4** shows details the mechanism of action for the acridine derivatives synthesis.



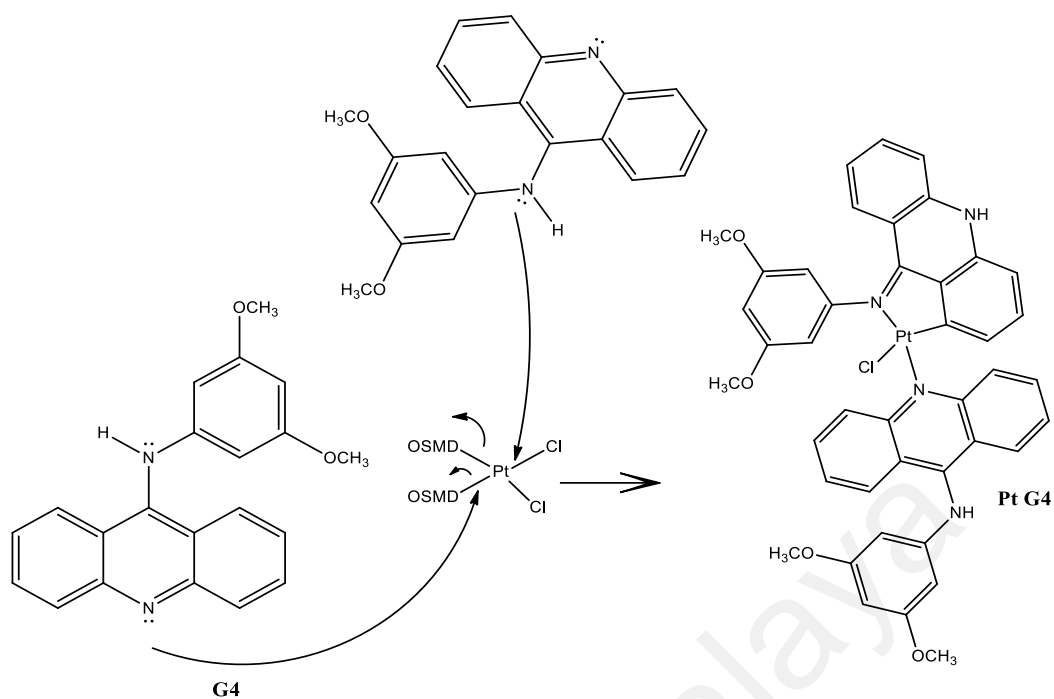
**Scheme 4.4:** Mechanism of the synthesis acridine derivatives

The Pt complexes were obtained with the acridine as ligand. The coordination was between the lone pair of electrons owned by the N atom at the heterocyclic counterpart and not from the amine moiety. The **Pt G3** and **Pt G7** complexes were found to be in this condition and owned a tetrahedral geometry. **Scheme 4.5** shows the mechanism of platinum complexes of **Pt G3** and **Pt G7**



**Scheme 4.5:** Mechanism of platinum complexes of Pt G3 and Pt G7

The organometallic (Jamali et al., 2008) complex, **Pt G4** was shown in **Scheme 4.6**, which the formation of **Pt G4** occurred by chelating the two nitrogen atoms with two ligands **G4**. The square planar appear in this complex with the organometallic bonding happens when the metal bind to the carbon ligand. **G4** is relatively bulky as compared to other synthesized ligands. The bulkier amine and the presence of methyl group as a donor electron might be decisive in promoting the cyclometalation. The steric hindrance will promote the cycloplatination especially for primary amine (Gallego et al., 2007; Martín et al., 2009).



**Scheme 4.6:** Mechanism of platinum complex of Pt G4

## 4.2 General and spectroscopic characterization ligands and complexes of acridine derivatives

**Table 4.1** shows the colour, percentage yield and elemental analysis data of acridine derivatives with its platinum complexes. The elemental analysis of C, H and N was compared to its theoretical value and found that the experimental data was in good agreement with the proposal formulae.

**Table 4.1:** Physical properties and analytical data of acridine derivatives and their Pt (II) complexes

Compound	Colour	Percentage yield (%)	Elemental percentage (%)		
			found (calculated)		
			C	H	N
<b>G3</b>	Yellow	76.0	84.41 (84.42)	5.42 (5.22)	10.42 (10.36)
<b>Pt G3</b>	Brownish orange	51.0	38.98 (41.05)	2.65 (3.28)	4.34 (4.56)
<b>G4</b>	Orange	91.8	75.96 (76.34)	5.26 (5.49)	8.79 (8.48)
<b>Pt G3</b>	Pale orange	53.1	40.80 (51.91)	3.69 (4.38)	4.42 (5.75)
<b>G7</b>	Pale yellow	58.1	79.33 (79.15)	4.88 (4.54)	9.34 (9.72)
<b>Pt G7</b>	Dark yellow	62.1	40.83 (41.91)	3.00 (3.36)	4.65 (4.44)

### 4.3 IR Spectral Data

The IR in **Table 4.2** shows the valuable information of the functional groups owned by the ligands and its complexes with in the frequencies range of 4000-400  $\text{cm}^{-1}$ .

The absorption band at  $\nu$  range of 3312.37 – 3460.52  $\text{cm}^{-1}$  can be assigned to the H-N group in acridine derivatives. The strong and sharp band of secondary amine clearly appeared in IR spectra of the ligands. The spectrum showed the appearance of an absorption band at  $\nu$  1568.26 - 1628.24  $\text{cm}^{-1}$  which can be assigned to the C=N group consist in acridine derivatives. Meanwhile, the IR spectra of the synthesized complexes showed some shifted in  $\nu$  due to the coordination of Pt(II) with the corresponding ligands. The absorption band at 2834.89 – 3124.79  $\text{cm}^{-1}$  was attributed to the aromatic group stretching that usually appeared stronger than bending. Nonetheless the weaker bending absorptions are useful to differentiate the similarity types of bond in aromatic substitution. The observed peak at the frequency of 750.79  $\text{cm}^{-1}$  suggesting the substitution at the aromatic group at ortho-position (Medapi et al., 2016; Mikata et al., 1998).

**Figure 4.1** shows the comparison of IR spectra between ligand **G3** and its Pt(II) complex, **Pt G3**. The shifting of the absorption frequencies were observed to be of C=N group from 1614.27  $\text{cm}^{-1}$  in **G3** to 1612.99  $\text{cm}^{-1}$  in **Pt G3** which indicates the evidence of the complexation reaction. A strong absorption appeared at 1266.72 – 1268.78  $\text{cm}^{-1}$  suggesting the C-S group absorption were not present in ligands but only in complexes, **Pt G3** and **Pt G7** suggesting a successful attachment of ligands to Pt centre. While for **G4** and **Pt G4**, a strong peak appeared at  $\nu$  1202.13 – 1203.51  $\text{cm}^{-1}$ , assigned to the C-O group.

The interaction between ligands and platinum was noticeably manifested in the IR spectrum. The range of complexation bands is not the same as its ligands but its depend on the origin of the vibration complex. The region of the acridine complexes in 400-1000

cm<sup>-1</sup> which corresponds to bending vibration of –Pt-N (Liu et al., 2016). Then,  $\nu(\text{Pt-N})$  vibration around  $\nu$  486.04 – 490.26 cm<sup>-1</sup>, indicates that the coordination of Pt(II) with ligands occur and the complexes were formed which was also influenced by doubly charged metal cation.

**Table 4.2:** Selected IR spectral data of acridine derivatives and their platinum (II) complexes

Compound	N-H	C=N	C=C	C-S	other	Pt-N
<b>G3</b>	3357.05	1614.27	1514.56	-	-	-
<b>Pt G3</b>	3312.37	1612.99	1500.07	1266.72	-	486.04
<b>G4</b>	3358.71	1614.16	1515.12	-	(C-O) 1170.33	-
<b>Pt G4</b>	3322.40	1568.26	1498.67	-	(C-Cl) 767.69	488.59
<b>G7</b>	3460.56	1628.24	1505.69	-	(C-F) 1219.52	-
<b>Pt G7</b>	3325.05	1614.21	1510.29	1268.78	(C-Cl) 756.01 (C-F) 1210.91	490.26

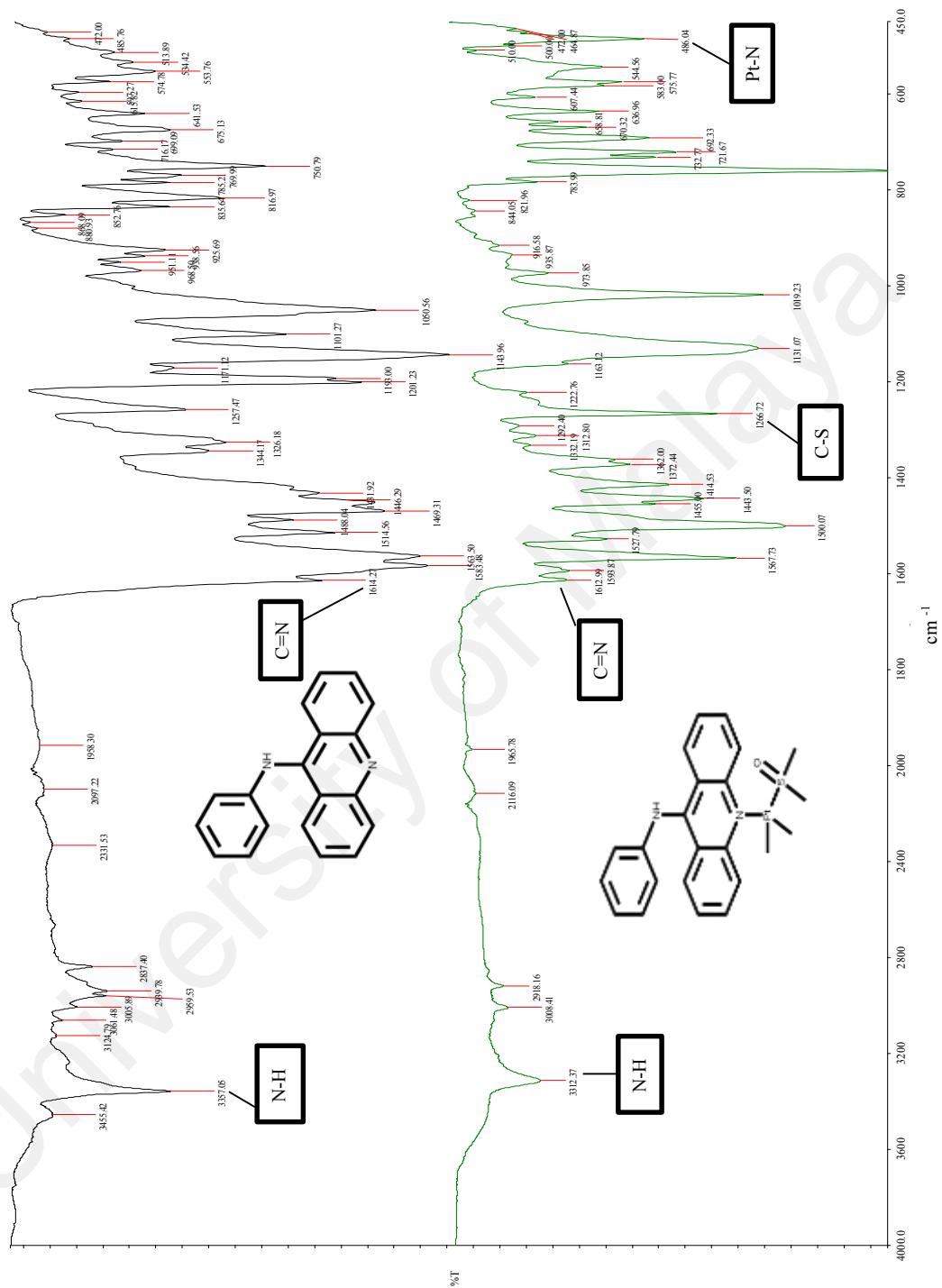


**Figure 4.1:** Comparison of IR spectra between ligand G3 and Pt (II) complex Pt G3

#### 4.4 <sup>1</sup>H NMR Spectral Data

The <sup>1</sup>H NMR spectra of the synthesized acridine derivatives ligands and their platinum complexes were recorded in chloroform-D or dimethylsulfoxide DMSO-*d*<sub>6</sub> using tetramethylsilane (TMS) as an internal standard. **Table 4.3** showed the <sup>1</sup>H NMR data of acridine derivatives and their platinum complexes.

The <sup>1</sup>H NMR data shows six singlet signals in the region  $\delta$  10.11-11.23 which could be assigned to N-H11 signals respectively. The H aromatic signals can be observed in the region of  $\delta$  6.23 – 8.20 ppm which can be attributed to the aromatic group owning a triplet and multiplet multiplicity. **Figure 4.2** showed <sup>1</sup>H NMR spectrum of *N*-phenylacridin-9-amine, **G3**. A couple of doublet signal for ligands and its Pt(II) complexes appeared at  $\delta$  7.12 – 9.82 ppm and  $\delta$  7.82 – 9.80 ppm were attributed to C-H1/8 and C-H4/5 proton of aromatic. The complexes are more deshielded compared to its ligand because of nitrogen atom coordinate to Pt(II) in complexes. The protons for methoxy group consist in **G4** appeared as sharp singlet peak at  $\delta$  3.64 ppm with integration corresponds to three protons. While methoxy group of **Pt G4** appeared at  $\delta$  3.49 and  $\delta$  3.62 with six protons absorbed due two ligands **G4** binds with Pt(II).

The H-N group in Pt(II) complexes were observed to have a slight shift due the coordination of metal to ligand. The differences of this peak between ligand and complexes is very significant. No proton peak was observed in the downfield region ( $>12.01$  ppm). **Figure 4.3** shows <sup>1</sup>H NMR spectrum of (*N*-phenylacridin-9-amine)*cis*-dichloro(dimethylsulfoxide)-platinum(II) **Pt G3**. There are two types of complexes which is one ligand one metal (L-M) and two ligands one metal (L-M-L). The formation of complexes depends on the steric of its ligands and also the solvent used.

**Table 4.3:** Selected  $^1\text{H}$  NMR data of acridine derivatives and their platinum (II) complexes

Compound	Position ( $\delta$ )				
	1/8	4/5	11	Other functional group	Ar-H
<b>G3</b>	8.01	8.10	11.03	-	7.51, 7.39, 7.37, 7.29, 7.00
<b>Pt G3</b>	8.17	9.83	10.20	-	8.03, 7.43, 7.32, 7.12, 7.05
<b>G4</b>	8.16	8.26	11.02	3.64 (-OCH <sub>3</sub> )	7.45, 7.10, 6.56, 6.23
<b>Pt G4</b>	9.72	9.82	10.11	3.62, 3.49 (-OCH <sub>3</sub> )	8.20, 8.00, 7.48, 6.27, 6.19, 6.14
<b>G7</b>	7.12	7.82	11.23	-F	7.50, 7.00, 6.83
<b>Pt G7</b>	8.15	9.80	10.18	-F	7.98, 7.45, 7.20

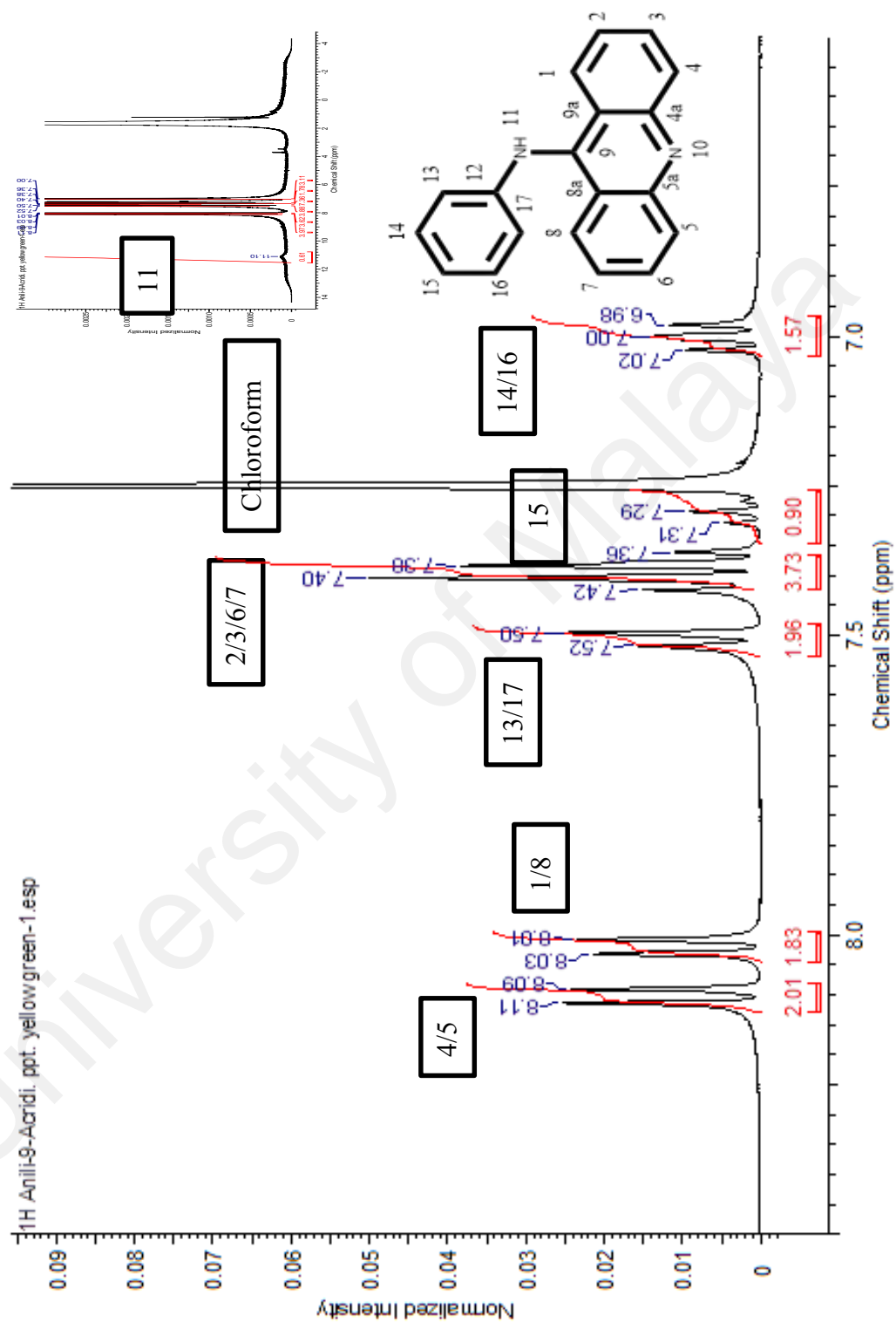
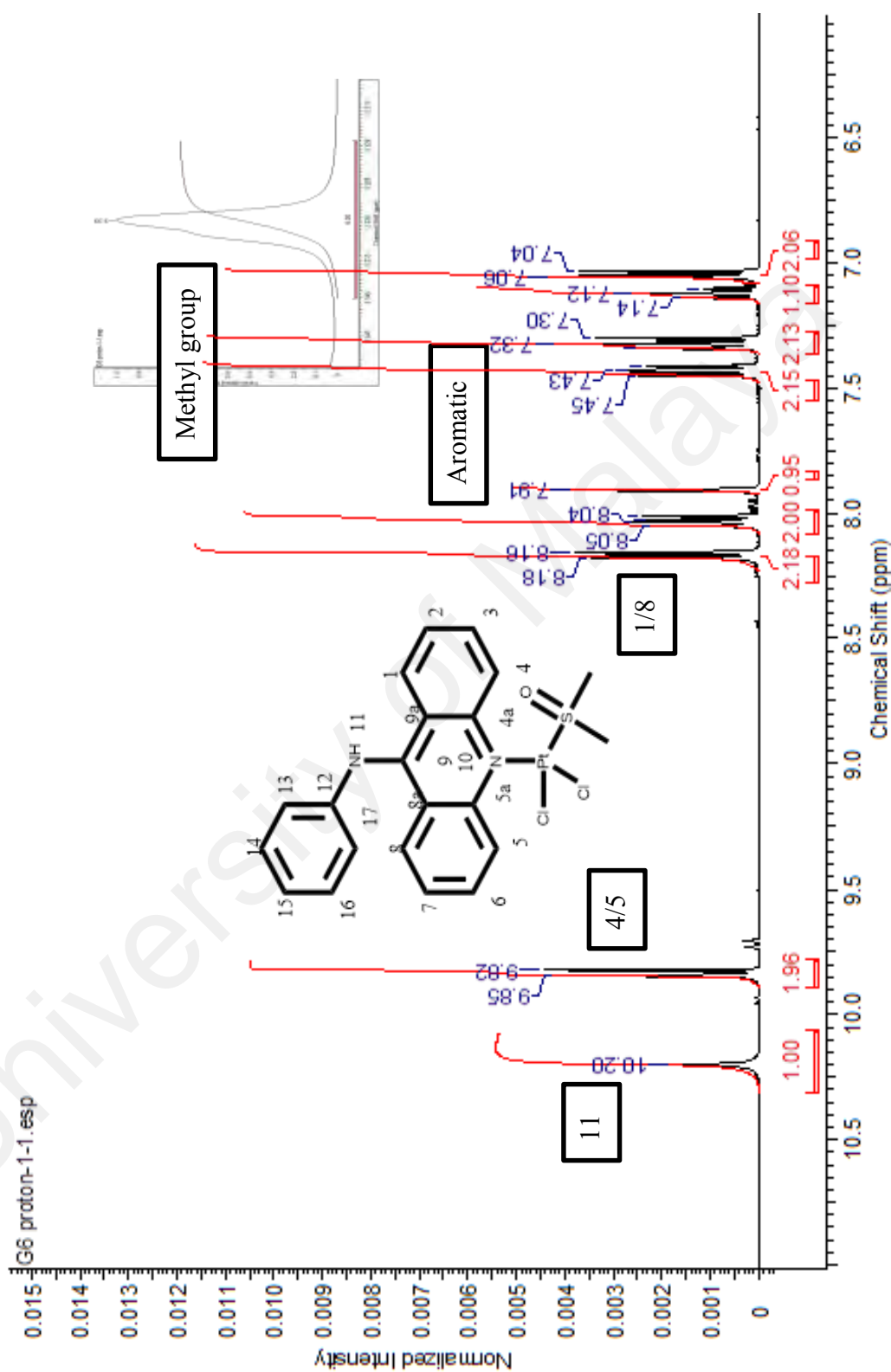


Figure 4.2:  $^1\text{H}$  NMR spectrum of N-phenylacridin-9-amine, G3 (400 MHz, chloroform-D)



**Figure 4.3:**  $^1\text{H}$  NMR spectrum of (N-phenylacridin-9-amine) cis-dichloro (dimethylsulfoxide) platinum(II), Pt G3 (400 MHz,  $\text{DMSO-d}_6$ )

## 4.5 <sup>13</sup>C NMR Spectral Data

**Table 4.4** shows the <sup>13</sup>C NMR data of the acridine derivatives ligands and their platinum complexes. The most downfield peak at  $\delta$  150.32 – 189.58 ppm was due to the electronegativity effects of nitrogen atom in the complexes due to the coordination of Pt(II) (C-N-Pt).

From the table, we can see clearly the shifting between ligands and complexes. The more deshielded peak of **G7** and **Pt G7** at  $\delta$  160.39-191.83 ppm shows the carbon atom at fluorine as a functional group. For the functional group of **G4** and **Pt G4** which is methoxy, the carbon atom signal appeared at the most downfield region,  $\delta$  161.62-161.64 ppm. The parent skeleton of acridine consists of four quaternary carbon at position 8a/9a, 4a/5a, 9 and 12 within range  $\delta$  114.78 – 189.58 ppm. **Figure 4.4** showed <sup>13</sup>C APT NMR spectrum of *N*-phenylacridin-9-amine, **G3**. The difference between <sup>13</sup>C APT NMR and <sup>13</sup>C NMR is positive signal shows methine and methyl group, while negative signals attributed to methylene and quaternary carbon group. This technique however is less sensitive than DEPT.

The carbon atom of aromatic ring signal appeared at  $\delta$  96.31 - 148.08 ppm which includes primary, secondary and tertiary carbon. In **Pt G3**, the signal of –S-CH<sub>3</sub> was observed at  $\delta$  40.39 ppm, indicated that DMSO from Pt (II) salt binds to the **G3** ligand. The <sup>13</sup>C NMR spectra of platinum complex, **Pt G3** (**Figure 4.5**) supported the <sup>1</sup>H NMR result and confirmed the formation of the complex. While the signal of –S-CH<sub>3</sub> in **Pt G7** at  $\delta$  44.45 ppm is slightly deshielded if compared to **Pt G3** might be due to the electronegativity of fluorine atom. However, in the **Pt G4** –S-CH<sub>3</sub> group peak not appear because DMSO already removed and substituted by another ligand **G4**.

**Table 4.4:** Selected  $^{13}\text{C}$  NMR Data of acridine derivatives and their platinum (II) complexes

Compound	Position ( $\delta$ )					
	8a/9a	4a/5a	9	12	Other functional group	Ar-C (-CH)
<b>G3</b>	114.89	150.32	142.30	137.79	-	134.32, 130.03, 126.94, 125.99, 123.87
<b>Pt G3</b>	118.91	150.83	148.49	144.06	40.39 (-S-CH <sub>3</sub> )	133.66, 132.81, 130.12, 128.58, 125.45, 124.67, 121.61
<b>G4</b>	114.78	154.32	142.81	139.95	161.62 (C-O-CH <sub>3</sub> ) 55.61 (-O-CH <sub>3</sub> )	134.49, 126.32, 123.91, 119.76, 101.91, 99.07
<b>Pt G4</b>	117.87	150.48	141.42	134.01	161.64 (C-O-CH <sub>3</sub> ) 55.78 (-O-CH <sub>3</sub> )	148.08, 145.91, 132.84, 128.42, 126.55, 125.38, 124.57, 121.55, 119.16, 99.64, 96.31
<b>G7</b>	117.88	158.03	152.98	141.41	160.39 (-C-F)	133.30, 126.96, 122.73, 126.26, 119.25, 117.05, 116.83
<b>Pt G7</b>	132.73	189.58	183.94	168.80	191.83 (-C-F) 44.45 (-S-CH <sub>3</sub> )	133.59, 128.60, 125.33, 124.63, 123.94, 117.00, 116.77

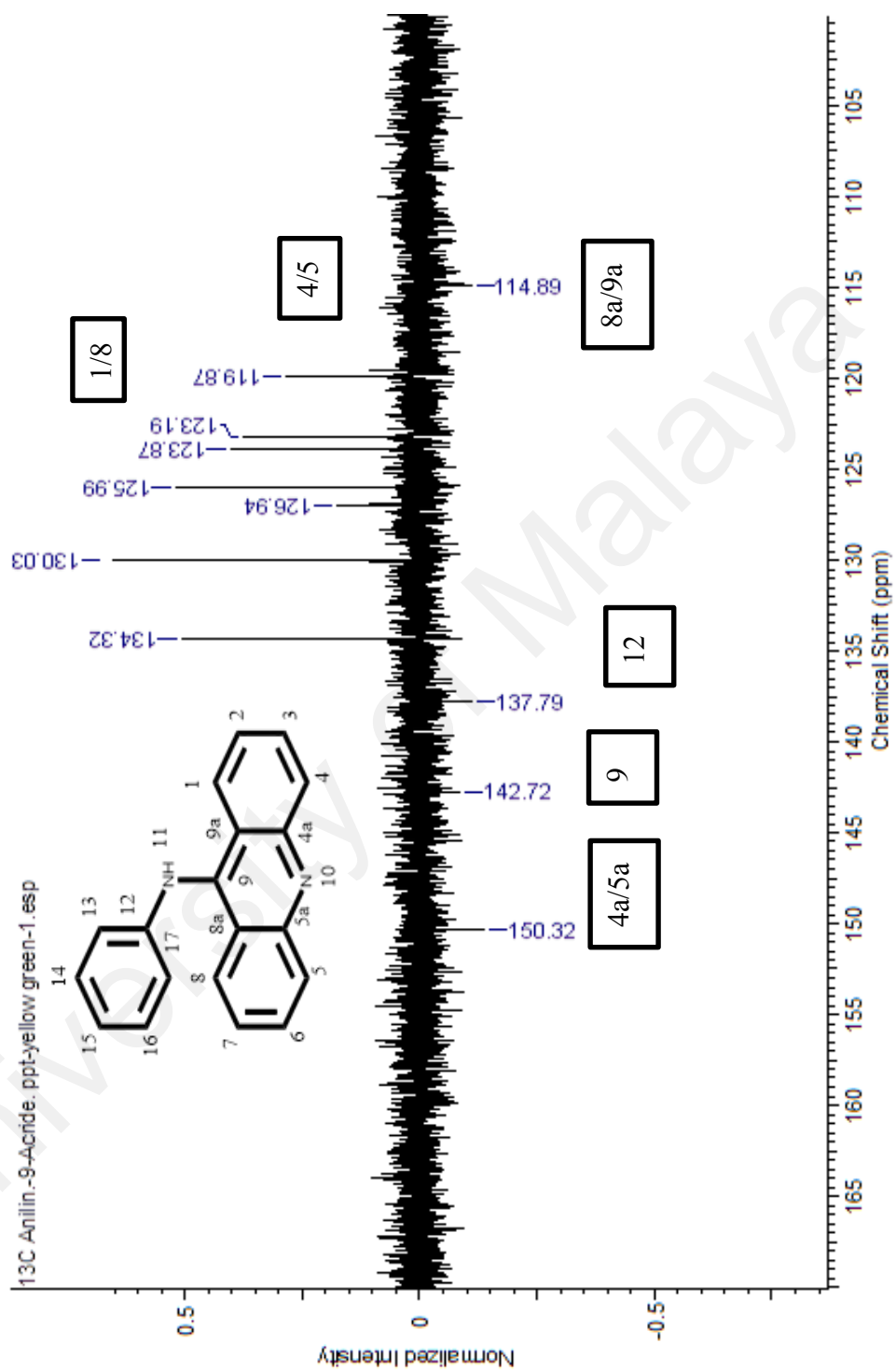


**Figure 4.4:** <sup>13</sup>C NMR spectrum of N-phenylacridin-9-amine, G3 (400 MHz, chloroform-D)

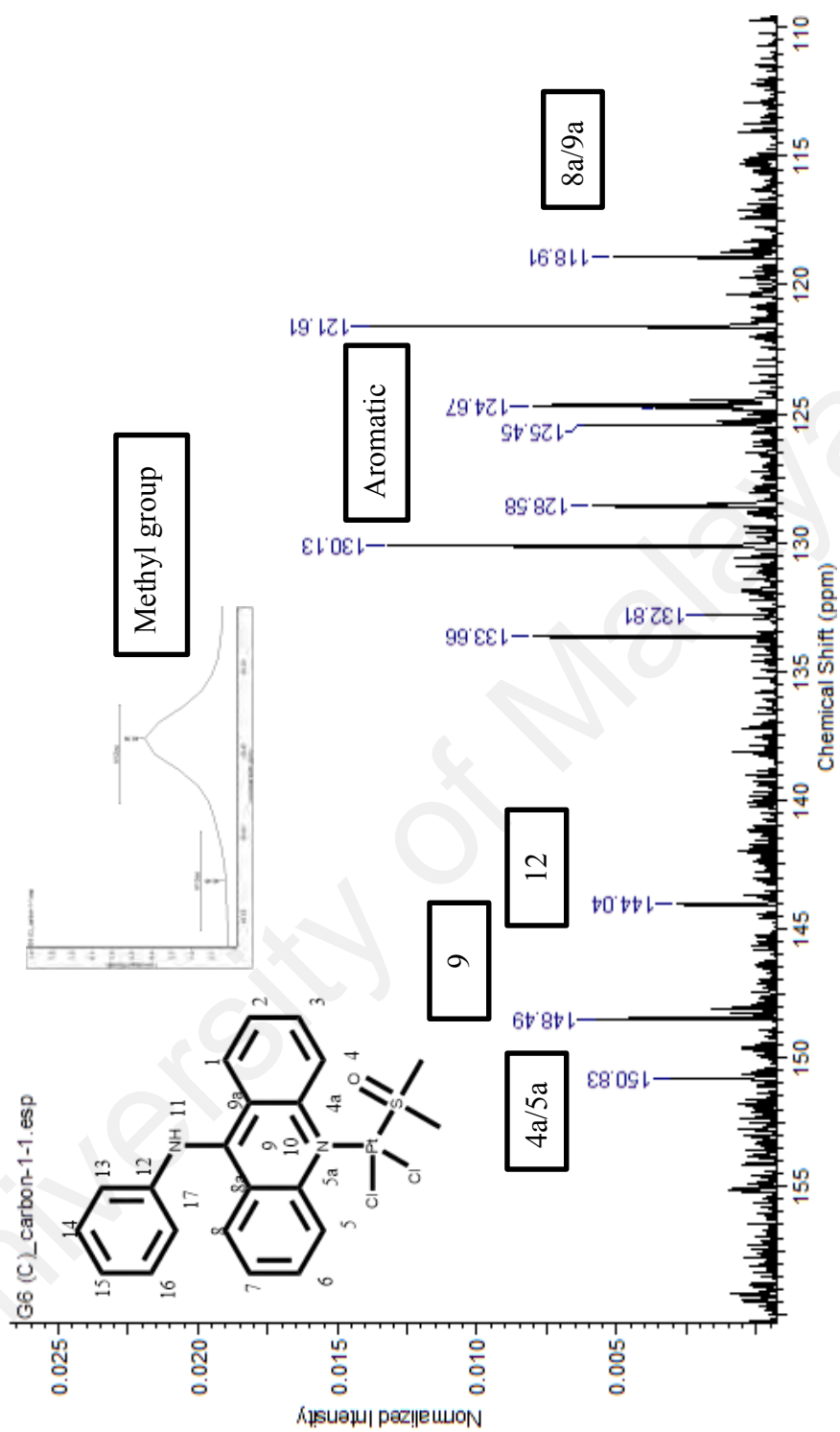


**Figure 4.5:**  $^{13}\text{C}$  NMR spectrum of (N-phenylacridin-9-amine) cis-dichloro (dimethylsulfoxide) platinum(II), Pt G3 (400 MHz, DMSO  $d_6$ )

## 4.6 X-ray Crystallographic Study

The crystal structures of three acridine derivatives **G4**, **Pt G3** and **Pt G4** were solved by using single crystal x-ray diffraction. These crystal were grown in different solvent due to the environment structural stability and also the steric nature of the compound. The dark brown crystal of **G3** was grown in ethanol with a few drop of triethylamine, but the crystal structure was known (Pang et al., 2014).

### 4.6.1 Crystal structure of G4

The structure of **G4** was determined by single crystal X-ray diffraction analysis and is found to be of discrete asymmetric units (**Figure 4.6**). The crystal data has been deposited to Cambridge Crystallographic Data Centre (CCDC) with the deposition number of CCDC 1587404. The crystallographic data and its structure refinement were collected and presented in **Table 4.5** In the **G4** molecule, 9-acridine (C13) is bound to 3,5-dimethoxyaniline (N1), as expected. The bond lengths and angles (**Table 4.6**) were in agreement with those of other associated derivatives in the literature (Jimenez et al., 2009; Solovyeva et al., 2016). The molecule can be divided into two main fragments: (C1-C13/N2) and (N1/C14-C21/O1/O2). The C1-C13/N2 and N1/C14-C21/O1/O2 planes were slightly planar, with a maximum deviation of C13 from the mean plane was 0.368(2). The dihedral angle between the aforementioned planes was 63.53(6)°. Also, there were no intra- or inter-hydrogen bonds in this molecule (**Figure 4.7**).

**Table 4.5:** Crystal data and structure refinement for G4

Identification code	Compound G4 from methanol
Empirical formula	C <sub>21</sub> H <sub>18</sub> N <sub>2</sub> O <sub>2</sub>
Crystal color	red
Formula weight	330.37
Temperature	293(2) K
Wavelength	1.54178 Å
Crystal system	Orthorhombic
Space group	P212121
a/Å	10.1753(4) Å
b/Å	11.8991(5) Å
c/Å	13.4416(6) Å
$\alpha$ /°	90.00
$\beta$ /°	90.00
$\gamma$ /°	90.00
Volume/ Å <sup>3</sup>	1627.47(12)
Z	4
$\rho_{\text{calc}}$ g/cm <sup>3</sup>	1.348 Mg/m
$\mu$ /mm <sup>-1</sup>	0.701 mm
F(000)	696
2 $\theta$ range for data collection/°	4.96 to 73.52
Index ranges	-11 ≤ h ≤ 12, -9 ≤ k ≤ 14, -15 ≤ l ≤ 16
Reflections collected	4381
Independent reflections	2819 [R(int) = 0.0410]
Data/restraints/ parameters	2819 / 0 / 227
Goodness of fit on F <sup>2</sup>	0.959
Final R indexes [I ≥ 2 $\sigma$ (I)]	R1 = 0.0551, wR2 = 0.1361
Final R indexes [all data]	R1 = 0.0541, wR2 = 0.1406
Largest diff. peak/hole / eÅ <sup>-3</sup>	0.496 and -0.368

**Table 4.6:** Selected bond length (Å) and angles (°)

Bond	Bond lengths (Å)	Bond	Bond angle (°)
C13-N1	1.287(3)	C13-N1-C14	123.0(2)
C14-N1	1.407(3)	C18-O1-C21	116.8(2)
C18-O1	1.369(3)	C16-O2-C20	117.2(2)
C16-O2	1.354(3)	N1-C13-C6	126.9(2)

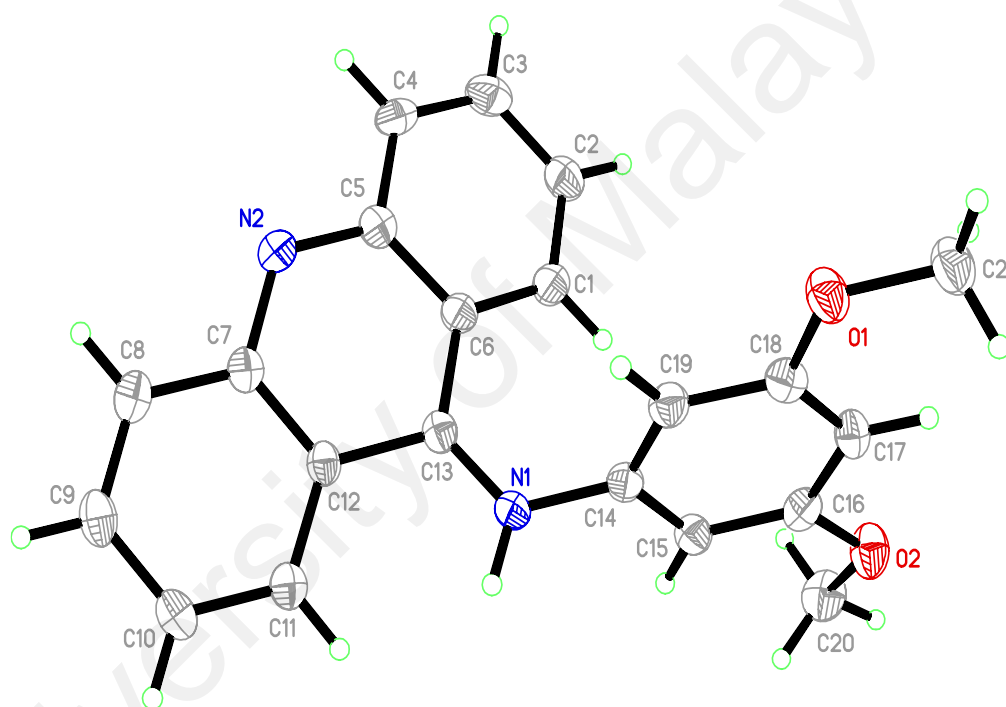


**Figure 4.6:** The ORTEP diagram of G4, showing 50% probability displacement ellipsoids and the atom-numbering scheme

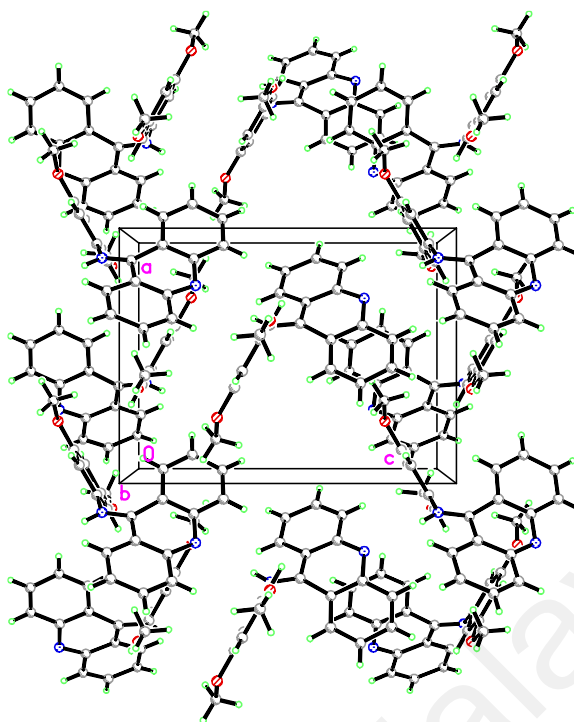


**Figure 4.7:** The packing of G4 viewed down to the b axis

#### 4.6.2 Crystal structure of Pt G3

The reaction of ligand, **G3** with  $\text{PtDMSO}_2\text{Cl}_2$  in 1:1 mol ratio resulting in the formation of the platinum complex **Pt G3** (*N*-phenylacridin-9-amine)*cis*-dichloro(dimethylsulfoxide)-platinum(II). The structure of the crystals grown in DMF, are shown in (**Figure 4.8**). The platinum metal bind to nitrogen N1 with the cisoid angle of  $88.08^\circ$  and  $90.13^\circ$  with transoid angle atom. The Pt(II) is four coordination by one molecule from ligand in a distorted tetrahedral of  $90.09^\circ$  -  $91.70^\circ$  (Aghakhanpour et al., 2015; Cutillas et al., 2013; Eiter et al., 2009). The selected bond lengths and bond angles are given in **Table 4.7** and the crystal data and structural refinement were listed in **Table 4.8**.

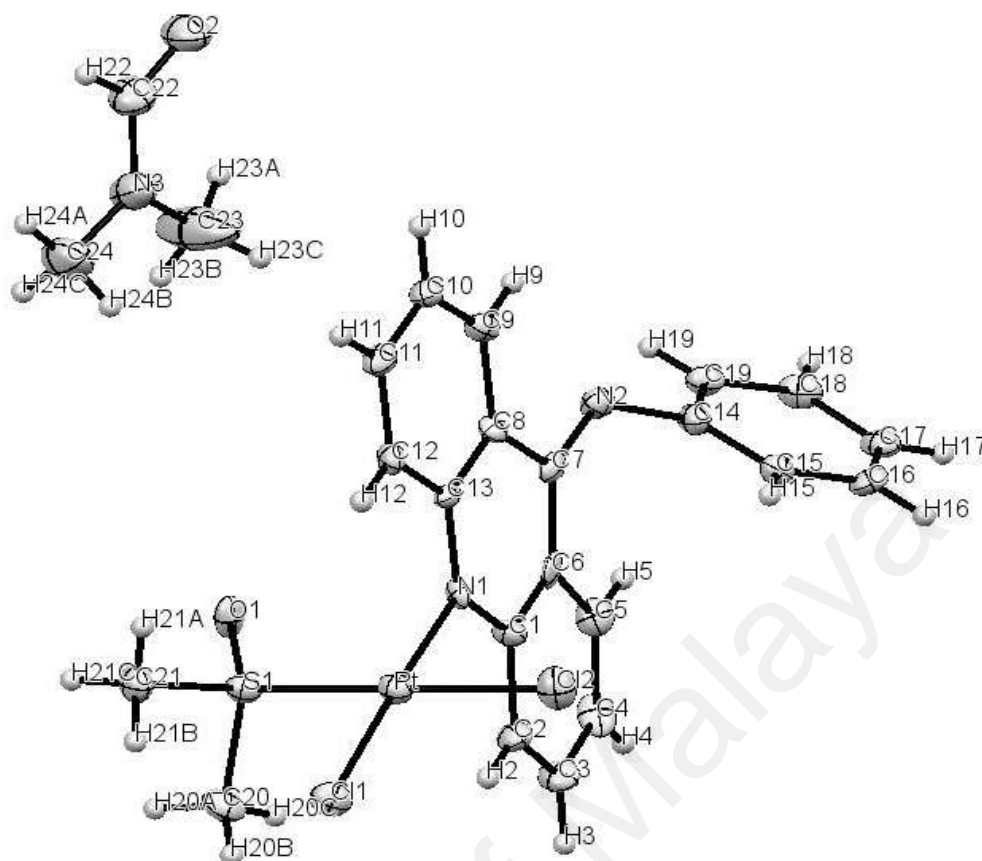


**Figure 4.8:** The crystal structure of platinum complex, Pt G3 ORTEP

#### 4.6.3 Crystal structure of Pt G4

The reaction of ligand **G4** with  $\text{PtDMSO}_2\text{Cl}_2$  in 1:1 mol ratio to resulting in the formation the platinum complex **Pt G4**, (*N*-(3,5-dimethoxyphenyl)acridin-9-amine)*cis*-dichloro(dimethylsulfoxide)-platinum(II). The structure of the crystal grown in DMSO, are shown in **Figure 4.9**. Platinum is  $d_{10}$  which is able to form four coordination, distorted tetrahedral. The platinum metal bind with two ligand at different position of nitrogen, N2 and N3 (Ceci et al., 1996). The four coordination with platinum is three from ligand with the cisoid angle of  $94.35^\circ$  and  $94.67^\circ$  with transoid angle atom. The selected bond lengths and bond angles are given in **Table 4.7** and the crystal data and structural refinement were listed in **Table 4.8**.

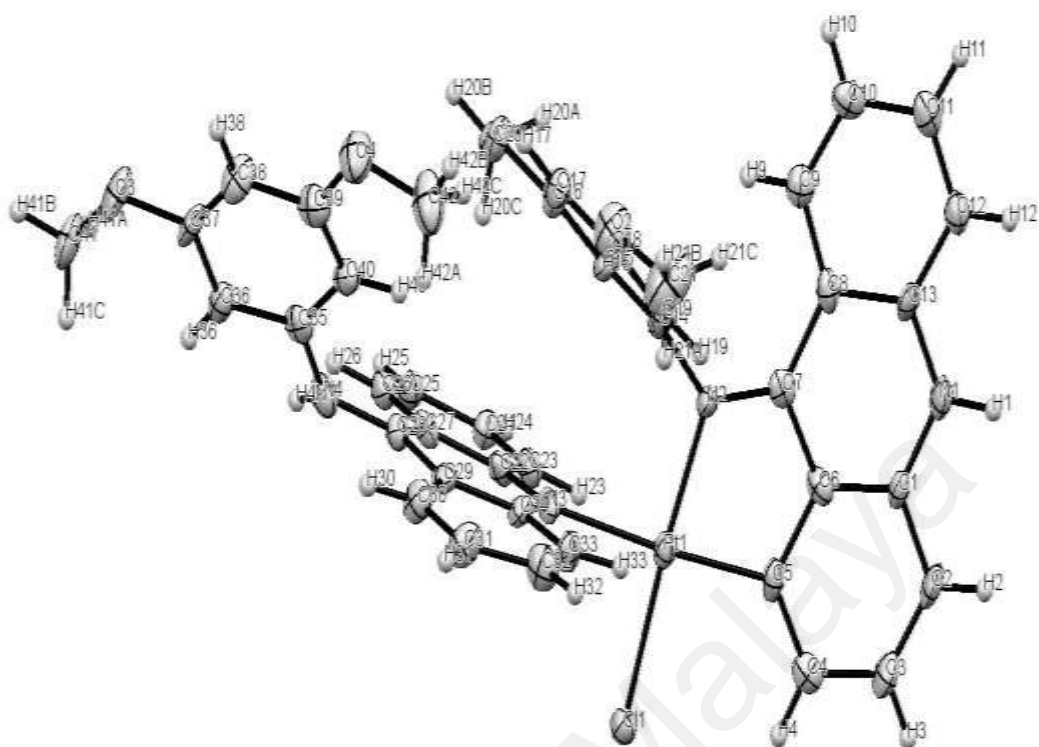


**Figure 4.9:** The crystal structure of platinum complex, Pt G4 ORTEP

University of Malaysia

**Table 4.7:** Selected bond length (Å) and bond angles (°) for the Pt G3 and Pt G4 complexes

<b>Pt G4</b>		<b>Pt G3</b>	
<b>Bond length (Å)</b>		<b>Bond length (Å)</b>	
Pt1 – C5	1.992	Pt – Cl1	2.320
Pt1 – Cl1	2.328	Pt – Cl2	2.305
N1 – H1	0.924	Pt – N1	2.072
N2 – Pt1	2.017	Pt – S1	2.199
N3 – Pt1	2.149	C14 – N2	1.435
N2 – C14	1.436	N2 – C7	1.354
N2 – C7	1.329	C13 – N1	1.353
N3 – C34	1.367	N1 – C1	1.370
N4 – H4N	0.783	S1 – C21	1.781
C35 – N4	1.413	S1 – O1	1.443
C28 – N4	1.376	C21 – H21B	0.960
C39 – O4	1.379	N1 – H2	2.598
C42 – O4	1.379	N2 - H9	2.546
C16 – O1	1.366	<b>Bond angle (°)</b>	
C20 – O1	1.435	C14 – N2 – C7	125.14
C21 – O2	1.415	C1 – N1 – C13	120.62
C18 – O2	1.367	N1 – Pt – Cl2	88.08
C37 – O3	1.371	Cl1 – Pt – S1	90.13
C41 – O3	1.425	O1 – S1 – C20	107.21
C41 – H41B	0.961	N1 – C1 – C2	119.17
C21 – H21B	0.960	N1 – C13 – C12	119.36
C20 – H20A	0.960	C5 – C6 – C7	124.45
<b>Bond angle (°)</b>		C7 – C8 – C9	122.47
C35 – N4 – C28	128.62	C20 – S1 – C21	100.92
C7 – N2 – Pt1	116.51		
C1 – Pt1 – C5	94.35		
N3 – Pt1 – N2	94.67		
Cl3 – N1 – H1	124.05		
C21 – O2 – C18	117.64		
C39 – O4 – C42	116.84		
C37 – O3 – C41	116.56		
C34 – N3 – C22	118.22		

**Table 4.8:** Crystal data and structure refinement of Pt G3 and Pt G4 complexes

Identification code	Compound Pt G4 from DMSO	Compound Pt G3 from DMF
<b>Empirical formula</b>	C <sub>42</sub> H <sub>35</sub> Cl N <sub>4</sub> O <sub>4</sub> Pt	C <sub>24</sub> H <sub>26</sub> Cl <sub>2</sub> N <sub>3</sub> O <sub>2</sub> Pt S
<b>Crystal size (mm)</b>	0.3000 x 0.2500 x 0.0200	0.5300 x 0.2500 x 0.2000
<b>Crystal color</b>	orange	orange block
<b>Formula weight</b>	890.28	686.53
<b>Temperature</b>	293(2) K	100.2(8) K
<b>Wavelength</b>	0.71073	0.71073
<b>Crystal system</b>	Monoclinic	Triclinic
<b>Space group</b>	P 1 21/n	P 1
<b>a/Å</b>	9.7803(4)	7.8322(2)
<b>b/Å</b>	24.7870(14)	12.8710(4)
<b>c/Å</b>	14.3144(7)	13.1753(5)
<b>α/°</b>	90.00	95.454(3)
<b>β/°</b>	90.094(4)	96.121(3)
<b>γ/°</b>	90.00	107.150(3)
<b>Volume/ Å<sup>3</sup></b>	3470.2(3)	1250.65(7)
<b>Z</b>	4	2
<b>ρ<sub>calc</sub> g/cm<sup>3</sup></b>	1.704 Mg/m	1.823 Mg/m
<b>μ/mm<sup>-1</sup></b>	4.172 mm	5.934 mm
<b>F(000)</b>	1768	670
<b>2θ range for data collection/ °</b>	2.846 to 29.538	3.076 to 29.434
<b>Index ranges</b>	-11 ≤ h ≤ 12, -34 ≤ k ≤ 25, -17 ≤ l ≤ 19	-10 ≤ h ≤ 10, -16 ≤ k ≤ 16, -18 ≤ l ≤ 18
<b>Reflections collected</b>	18775	21485
<b>Independent reflections</b>	7585 [R(int)=0.0480]	6178 [R(int) = 0.0605]
<b>Data/restraints/parameters</b>	7585/0/479	6178 / 0 / 302
<b>Goodness of fit on F<sup>2</sup></b>	1.071	1.042
<b>Final R indexes [I ≥ 2σ (I)]</b>	R1 = 0.0412, wR2 = 0.0799	R1 = 0.0902, wR2 = 0.2054
<b>Final R indexes [all data]</b>	R1 = 0.0607, wR2 = 0.0955	R1 = 0.1005, wR2 = 0.2140
<b>Largest diff. peak/hole / eÅ<sup>-3</sup></b>	1.635/-1.276	20.959/-3.088

Since the crystals does not appeared in any solvent up to this date for **G7** and **Pt G7** , the thermogravimetric analysis (TGA) were carried out under nitrogen with the heating rate of 20 °C per minute form 50 °C up to 900 °C. The TGA analysis of **G7** and **Pt G7** was shown in **Figure 4.10** and **Figure 4.11**, indicating that the **G7** was thermally stable up to 245 °C and the decomposition occurred completely without any residue at 700 °C with 99.78% of weight of **G7** decomposed. While, the thermal decomposition of **Pt G7**, was stable up to 300 °C and that thermal decomposition occurred and completely stop when reached 31.33% weight of **Pt G7**. About 68.01% of weight of **Pt G7** was burnt and the remaining residue was platinum oxide (PtO). The theoretical value of the PtO is 33.37% and the experimental show 31.99%. Thus, the results showed that the theoretical and the experimental of remaining product are typical and also the differences between ligand and its metal complex.

**Table 4.9:** The theoretical and the experimental of remaining product after decomposition process

<b>Compound</b>	<b>Theoretical value (%) (remaining product)</b>	<b>Experimental value (%) (remaining product)</b>
<b>Pt G3</b>	34.35	32.90
<b>Pt G4</b>	23.74	28.53
<b>Pt G7</b>	33.37	31.99

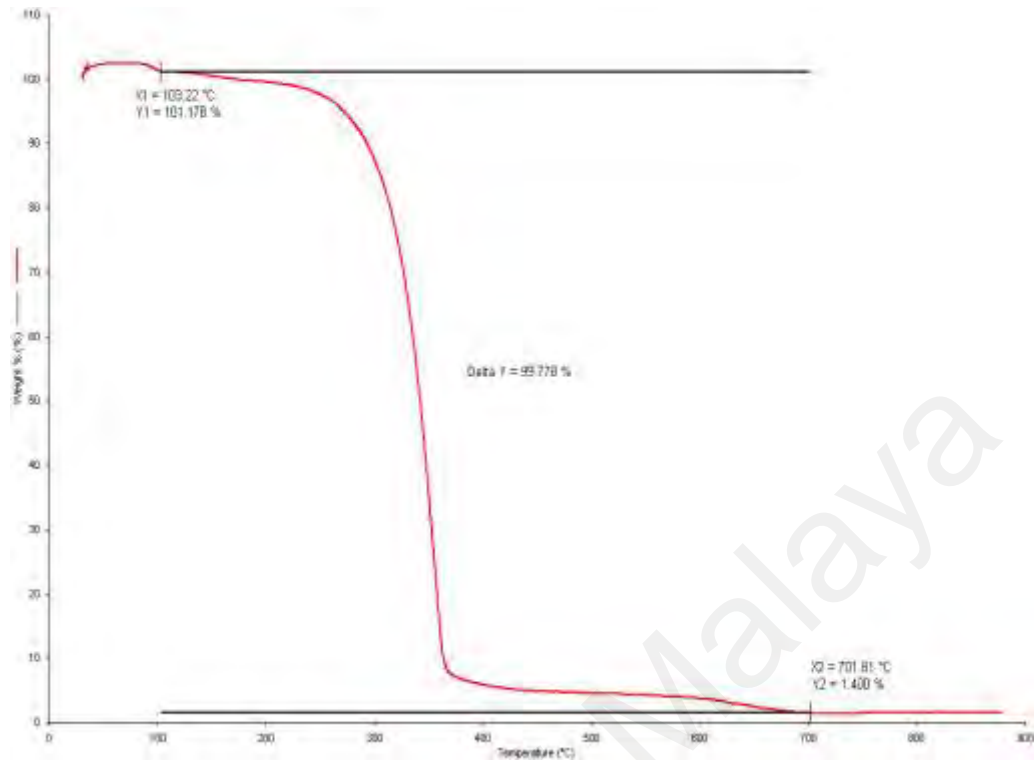


**Figure 4.10:** The TGA data of G7

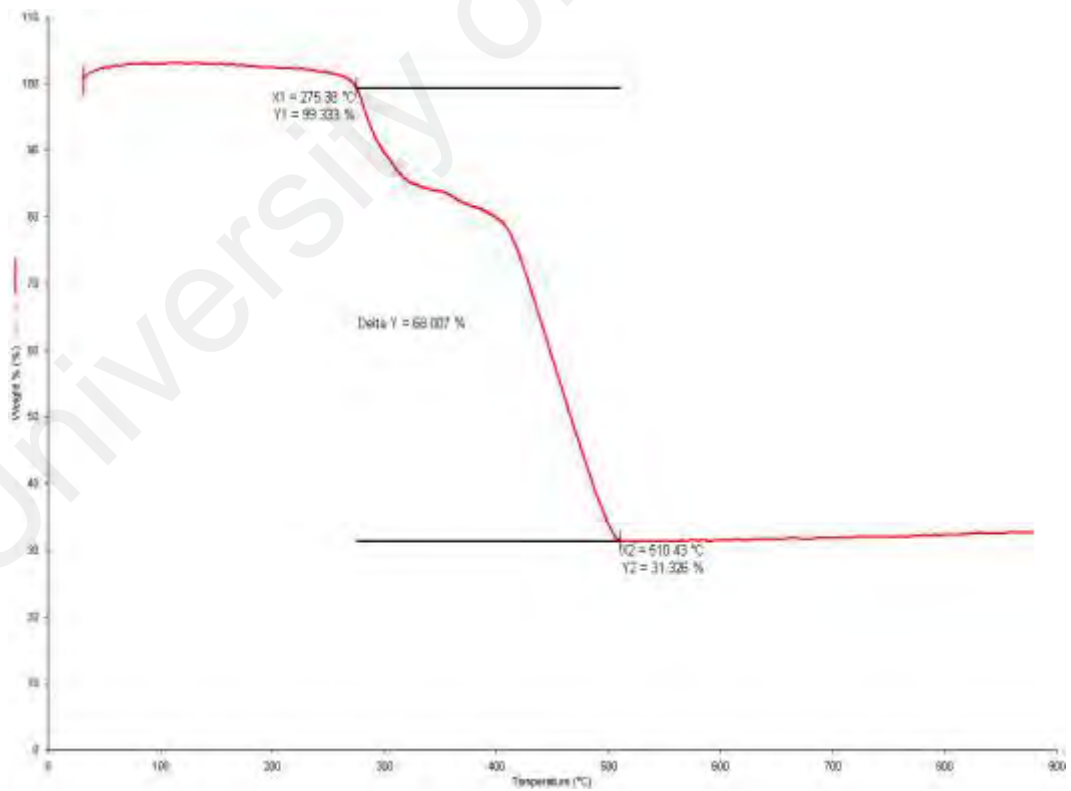


**Figure 4.11:** The TGA data of Pt G7

## 4.7 Biological activity

### 4.7.1 Anti-proliferative activity of compounds

The effects of compounds on the viability of MCF-7, HL60, HT29 and WRL68 cells were measured using the MTT assay. Cellular proliferation following 24 h of exposure to acridine derivatives and platinum complexes showed significant inhibition in **G3, G4, G7 Pt 3, Pt G4** and **Pt G7** -treated cells compared to non-treated cells (controls). As shown in **Table 4.10**, the  $IC_{50}$  of **G3, G4, G7 Pt 3, Pt G4** and **Pt G7** was following 24 h of treatment. The proliferation of all compound -treated cells decreased as the **G3, G4, G7 Pt 3, Pt G4** and **Pt G7** concentration increased. However, they exhibited no suppressive against normal WRL-68 hepatic cell compares to  $IC_{50}$  value of compounds toward viability of MCF-7, HL60 and HT29 cells. The  $IC_{50}$  value of WRL68 in this assay also recorded as positive as shown in **Table 4.10**. In the present research we have shown that the cytotoxic activities of **G3, G4, Pt G3** and **Pt G4** towards MCF-7, HT29 and HL60 cells are high while in the same time the toxicity against WRL68 was very low in treatment of **G3, G4, Pt G3** and **G7** while **Pt G4** and **Pt G7** are having toxicity against WRL68. The **G3** is good compound due to the result of  $IC_{50}$  value is low against MCF-7 and HL60 cells compared to other compounds. While the **G4** is good compound against HT29 and HL60 with the  $IC_{50}$  value below than 20  $\mu\text{g/mL}$ . This result considers as a beginning to study anti-cancer mechanism of **G3, G4, Pt G3** and **G7** towards all this cell line in the result above.

**Table 4.10:** Cytotoxicity effect of G3, G4, G7, Pt G3, Pt G4 and Pt G7

Cell line	IC <sub>50</sub> +SD (µg/mL)					
	G3	G4	G7	Pt G3	Pt G4	Pt G7
WRL68	56.0 ±	49.0 ±	50.0 ±	43.0 ±	29.0 ±	23.0 ±
	0.03	0.05	0.03	0.03	0.04	0.03
MCF-7	16.0 ±	22.0 ±	38.0 ±	18.5 ±	18.0 ±	42.5 ±
	0.05	0.04	0.05	0.03	0.03	0.03
HT29	22.0 ±	17.5 ±	-	24.0 ±	23.0 ±	-
	0.03	0.02	-	0.03	0.04	-
HL60	10.0 ±	15.0 ±	22.0 ±	13.5±	15.0 ±	19.5 ±
	0.04	0.03	0.04	0.04	0.05	0.04

#### 4.7.2 General acute toxicity observation for G4

The acute toxicity study was carried out to determine a nontoxic dosage for **G4**. After fourteen days of the intragastric administration of **G4** at two different concentrations, observed that there were no behavioral alterations or death was noticed. The investigation of compound **G4** towards the mice did not showed any abnormalities in term of their behaviors or physical appearances. Food and water was provided as usual and no abnormalities observed on their feces that were dark and dry. Other than that, there was also no significant differences in their body weight measurement between the mice.

**Table 4.11:** Serum biochemical data for male and female mice orally administered G4 at different concentration for 14 days.

<b>Parameters</b>	<b>Sex</b>	<b>Control mean <math>\pm</math> SD</b>	<b>Low dose mean <math>\pm</math> SD</b>	<b>High dose mean <math>\pm</math> SD</b>
<b>Sodium mmol/L</b>	Male	151 $\pm$ 1.22	152 $\pm$ 0.23	152.6 $\pm$ 3.13
	Female	149 $\pm$ 0.55	149.6 $\pm$ 0.54	149 $\pm$ 2.50
<b>Potassium mmol/L</b>	Male	5.8 $\pm$ 0.5	4.6 $\pm$ 1.4	5.01 $\pm$ 0.39
	Female	4 $\pm$ 0.7	4.84 $\pm$ 0.5	4 $\pm$ 1.21
<b>Chloride mmol/L</b>	Male	108.8 $\pm$ 1.64	107 $\pm$ 0.2	107.6 $\pm$ 2.30
	Female	110 $\pm$ 2.7	110.2 $\pm$ 1.1	109 $\pm$ 0.68
<b>Carbon Dioxide mmol/L</b>	Male	13.4 $\pm$ 4.5	13 $\pm$ 2.1	13.6 $\pm$ 2.90
	Female	19 $\pm$ 2.41	18 $\pm$ 2.9	19 $\pm$ 3.20
<b>Anion Gap mmol/L</b>	Male	34.8 $\pm$ 3.8	33.7 $\pm$ 0.9	35.2 $\pm$ 2.4
	Female	27 $\pm$ 0.55	27 $\pm$ 0.11	28.1 $\pm$ 1.89
<b>Urea mmol/L</b>	Male	8.26 $\pm$ 0.7	9 $\pm$ 0.76	8.86 $\pm$ 1.32
	Female	8 $\pm$ 0.8	8.8 $\pm$ 1.3	8.6 $\pm$ 1.2
<b>Creatinine mmol/L</b>	Male	8 $\pm$ 0	8 $\pm$ 0	8 $\pm$ 0
	Female	9 $\pm$ 0.5	9 $\pm$ 0.2	8 $\pm$ 0.23
<b>Albumin g/L</b>	Male	27.2 $\pm$ 2.6	28 $\pm$ 3.1	27 $\pm$ 1.2
	Female	27 $\pm$ 1.7	27 $\pm$ 0.24	28 $\pm$ 3.1
<b>Total Bilirubin umol/L</b>	Male	1 $\pm$ 0	1 $\pm$ 0	1.4 $\pm$ 0.55
	Female	1 $\pm$ 0.2	1 $\pm$ 0.23	1 $\pm$ 0.9
<b>Alkaline Phosphatase IU/L</b>	Male	61.4 $\pm$ 0.5	74 $\pm$ 0	75.2 $\pm$ 8.6
	Female	67 $\pm$ 6.5	68 $\pm$ 4.1	66.5 $\pm$ 3.7
<b>Alanine Aminotransferase IU/L</b>	Male	41.6 $\pm$ 0.9	41.1 $\pm$ 6.7	42.6 $\pm$ 3.2
	Female	34.01 $\pm$ 5.3	33.1 $\pm$ 0	33.4 $\pm$ 1.3
<b>G-Glutamyl Transferase IU/L</b>	Male	4.6 $\pm$ 3.2	4 $\pm$ 0.6	4.4 $\pm$ 1.82
	Female	2 $\pm$ 0.3	2 $\pm$ 0.21	3 $\pm$ 0.15

### 4.7.3 Serum biochemical parameters

All mice were treated with either 500 or 1000 mg/kg of compound **G4** did not exhibit significant differences in these hepatic markers. **Table 4.11** shows data of serum biochemical obtained. The level of serum albumin and total bilirubin did not show any significant changes. While the investigation was further with Alkaline Phosphatase (ALP), Alanine Aminotransferase (ALT) and Gamma-Glutamyl Transferase (GGT) on **G4** compound toward the liver function parameter. In addition, **Table 4.11** also shown there is no significant change in serum electrolyte such as potassium, chloride, sodium or urea. The mice were dosed with 500 mg/kg, male and female showed some significant increases in total cholesterol, high density lipoprotein cholesterol HDL, and low density lipoprotein cholesterol LDL and triglyceride level. While for the 1000 mg/kg treated mice, the results showed decreases in all parameter for male and female mice. The effect of **G4** on triglyceride, total cholesterol, HDL cholesterol and LDL cholesterol are shown in **Table 4.12**.

**Table 4.12:** The effect of G4 on triglyceride, total cholesterol, HDL cholesterol and LDL cholesterol.

Parameters	Sex	Control mean $\pm$ SD	Low dose mean $\pm$ SD	High dose mean $\pm$ SD
Triglyceride mmol/L	Male	1.54 $\pm$ 0.32	1.39 $\pm$ 0.33	1.16 $\pm$ 0.5
	Female	1.5 $\pm$ 0.4	1.8 $\pm$ 0.07	1.7 $\pm$ 0.41
Total Cholestrol mmol/L	Male	2.92 $\pm$ 0.41	3.1 $\pm$ 0.8	2.78 $\pm$ 0.3
	Female	2 $\pm$ 0.1	2.4 $\pm$ 0.13	2 $\pm$ 0.19
HDL Cholestrol mmol/L	Male	1.66 $\pm$ 0.32	1.8 $\pm$ 0.9	1.94 $\pm$ 0.5
	Female	0.9 $\pm$ 0.27	2.4 $\pm$ 0.13	1.2 $\pm$ 0.26
LDL Cholestrol mmol/L	Male	1.21 $\pm$ 0.2	1.13 $\pm$ 0.69	1.48 $\pm$ 0.72
	Female	1.53 $\pm$ 0.1	1.67 $\pm$ 0.74	1.37 $\pm$ 0.49

#### 4.7.4 Histopathological evaluation

The kidney and liver examination of the mice did not show any abnormalities in gross appearances and weight as a results of the compound consumption. The results from the gross examination were also confirmed by histopathological assessment. There were no detected ion of any damages in their gastrointestinal tracts or the potential and direct target for toxic effects of the ingested foods. **G4** was also found to not implicatory any significant histological changes in the organ tissues of any of the mice (**Figure 4.12**). Hence, it can be concluded that there were no necrosis, cirrhosis or inflammation was observed. These outcomes revealed that **G4** up to an intragastric concentration of 1000 mg/kg was not-toxic in rats.

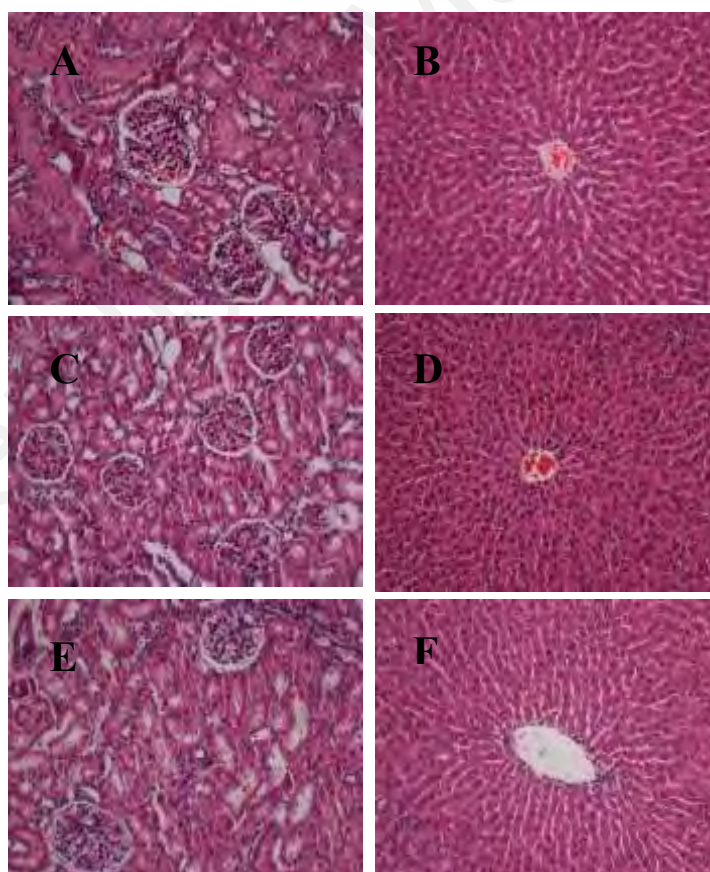


**Figure 4.12:** Effect of G4 compound on histological sections of the liver and kidney in rats. (A, B) Rats treated with vehicle. (C, D) Rats treated with 500 mg/kg of G4. (E, F) Rats treated with 1000 mg/kg of G4. (H &E stain, 20× magnifications)

## CHAPTER 5: CONCLUSION

A new series of platinum complexes with acridine derivatives **Pt G3**, **Pt G4** and **Pt G7** were synthesized using the ligands **G3**, **G4** and **G7**. The **G4** is a new and novel ligand from acridine derivatives derived from 3,5 dimethoxyaniline and 2-chlorobenzoic acid as a precursor. The percentages yields of complexes were about 50-60% as compared to its ligand. A higher percentages yield (90%) was obtained for **G4**. The platinum was bound to N as donor atom, to form complex with a distorted tetrahedral geometry. The crystal structure of **Pt G3** showed that the type of metal-ligand referred as monodentate due to the lone pair electron shared between the N atom and Pt(II) atom. While for the crystal structure of **Pt G5**, the organometallic cycloplatinum was found to be the type of chelate with two ligand and one metal (monodentate). Two ligands (**G4**) were bond to the Pt(II) to form **Pt G4** from N(2) and N(3) atoms as showed in crystal structure. The N(2) atom came from the acridine skeleton itself and another nitrogen atom N(3) is from the substituent (3,5 dimethoxyaniline). The only of difference between **Pt G3** and **Pt G4** is the bonding of C(5) with the platinum. The cyclometallate of the ligand also effected by the steric and basicity of the ligand. The bulky of ligand or primary amine will ease in promoting the cycloplatination.

All the synthesized compounds **G3**, **G4**, **G7**, **Pt G3**, **Pt G4** and **Pt G7**, had shown good anticancer activities against MCF-7, HT29 and HL60 cells. From MTT assay, the cytotoxic activities of compound towards MCF-7, HT29 and HL60 cells were low in  $IC_{50}$  values. However, the value of  $IC_{50}$  for WRL68 was very high in treatment using the synthesized compounds indicated that it is harmless for normal cells. The HL60 cell showed the best result by treatment of all compounds which was less than 20  $\mu\text{g/mL}$  ( $IC_{50}$  value) as compared to other cells. While for acute toxicity test of **G4**, the histopathological evaluations for the liver and kidney as well as the serum biochemistry

results in which no indications of toxicity were noticed after intragastric administration of the 2 concentrations of MDLA. From that we can say, **G4** up to an intragastric concentration of 1000 mg/kg was not-toxic in rats.

### **5.1 Future work**

Further investigations on biological important of these compound can be carried out. The study of the reaction mechanisms of those compounds toward cancer cell is also a consideration for further discovering. The acute toxicity study can be conducted to the remaining compounds and further research in the area of *in vivo* studies might be vital for the development of new pharmaceuticals drugs.

University of Malaya

## REFERENCES

- Aghakhanpour, R. B., Nabavizadeh, S. M., Rashidi, M., & Kubicki, M. (2015). Luminescence properties of some monomeric and dimeric cycloplatinated(ii) complexes containing biphosphine ligands. *Dalton Transactions*, 44 (36), 15829-15842.
- Aguirre, P. A., Lagos, C. A., Moya, S. A., Zuniga, C., Vera-Oyarce, C., Sola, E., Peris, G., & Bayon, J. C. (2007). Methoxycarbonylation of olefins catalyzed by palladium complexes bearing P,N-donor ligands. *Dalton Transactions* (46), 5419-5426.
- Aitken, D. J., Albinati, A., Gautier, A., Husson, H.-P., Morgant, G., Nguyen-Huy, D., Kozelka, J., Lemoine, P., Onger, S., Rizzato, S., & Viossat, B. (2007). Platinum(II) and Palladium(II) Complexes with N-Aminoguanidine. *European Journal of Inorganic Chemistry*, 2007 (21), 3327-3334.
- Almeida, S. M. V. d., Lafayette, E. A., Silva, W. L., Lima Serafim, V. d., Menezes, T. M., Neves, J. L., Ruiz, A. L. T. G., Carvalho, J. E. d., Moura, R. O. d., Beltrão, E. I. C., Carvalho Júnior, L. B. d., & Lima, M. d. C. A. d. (2016). New spiro-acridines: DNA interaction, antiproliferative activity and inhibition of human DNA topoisomerases. *International Journal of Biological Macromolecules*, 92, 467-475.
- Auparakkitanon, S., & Wilairat, P. (2000). Cleavage of DNA induced by 9-anilinoacridine inhibitors of topoisomerase II in the malaria parasite *Plasmodium falciparum*. *Biochemical and Biophysical Research Communications*, 269 (2), 406-409.
- Ba-gen, N., Chen, Y.-L., Baderihu, Tong, Y.-F., Ye Ri, G., & Wang, Q.-H. (2014). Two new xanthenes from *Lomatogonium carinthiacum*. *Chinese Journal of Natural Medicines*, 12 (9), 693-696.
- Bacherikov, V. A., Chang, J.-Y., Lin, Y.-W., Chen, C.-H., Pan, W.-Y., Dong, H., Lee, R.-Z., Chou, T.-C., & Su, T.-L. (2005). Synthesis and antitumor activity of 5-(9-acridinylamino)anisidine derivatives. *Bioorganic & Medicinal Chemistry*, 13 (23), 6513-6520.
- Becka, M., Vilková, M., Salem, O., Kaspariková, J., Brabec, V., & Kozurková, M. (2017). 3-[(E)-(acridin-9'-ylmethylidene)amino]-1-substituted thioureas and their biological activity. *Spectrochimica Acta Part A: Molecular and Biomolecular Spectroscopy*, 180, 234-241.
- Benoit, A. R., Schiaffo, C., Salomon, C. E., Goodell, J. R., Hiasa, H., & Ferguson, D. M. (2014). Synthesis and evaluation of N-alkyl-9-aminoacridines with antibacterial activity. *Bioorganic and Medicinal Chemistry Letters*, 24 (14), 3014-3017.
- Borovlev, I. V., Demidov, O. P., Amangasieva, G. A., & Avakyan, E. K. (2016). Direct and facile synthesis of 9-aminoacridine and acridin-9-yl-ureas. *Tetrahedron Letters*, 57 (32), 3608-3611.

- Budzisz, E., Malecka, M., Keppler, B. K., Arion, V. B., Andrijewski, G., Krajewska, U., & Rozalski, M. (2007). Synthesis, Structure, Protolytic Properties, Alkylating and Cytotoxic Activity of Novel Platinum(II) and Palladium(II) Complexes with Pyrazole-Derived Ligands. *European Journal of Inorganic Chemistry* (23), 3728-3735.
- Caffrey, C. R., Steverding, D., Swenerton, R. K., Kelly, B., Walshe, D., Debnath, A., Zhou, Y.-M., Doyle, P. S., Fafarman, A. T., Zorn, J. A., Land, K. M., Beauchene, J., Schreiber, K., Moll, H., Ponte-Sucre, A., Schirmeister, T., Saravanamuthu, A., Fairlamb, A. H., Cohen, F. E., McKerrow, J. H., Weisman, J. L., & May, B. C. H. (2007). Bis-acridines as lead antiparasitic agents: structure-activity analysis of a discrete compound library in vitro. *Antimicrobial Agents and Chemotherapy*, 51 (6), 2164-2172.
- Ceci, E., Cini, R., Konopa, J., Maresca, L., & Natile, G. (1996). Coordination and pericarbon metalation of 1-nitro-9-[(2-aminoethyl) amino] acridines toward platinum (II). evidences for hydrogen bonding between endocyclic N (10) H and chloride ion. *Inorganic Chemistry*, 35 (4), 876-882.
- Chandra, T., Garg, N., Lata, S., Saxena, K. K., & Kumar, A. (2010). Synthesis of substituted acridinyl pyrazoline derivatives and their evaluation for anti-inflammatory activity. *European Journal of Medicinal Chemistry*, 45 (5), 1772-1776.
- Chang, J.-Y., Lin, C.-F., Pan, W.-Y., Bacherikov, V., Chou, T.-C., Chen, C.-H., Dong, H., Cheng, S.-Y., Tasi, T.-J., Lin, Y.-W., Chen, K.-T., Chen, L.-T., & Su, T.-L. (2003). New analogues of AHMA as potential antitumor agents: synthesis and biological activity. *Bioorganic & Medicinal Chemistry*, 11 (23), 4959-4969.
- Chen, J., Cao, X., An, Q., Zhang, Y., Li, K., Yao, W., Shi, F., Pan, Y., Jia, Q., Zhou, W., Yang, F., Wei, F., Wang, N., & Yu, B. (2018). Inhibition of cancer stem cell like cells by a synthetic retinoid. *Nature Communications*, 9 (1), 1406.
- Chen, C.-H., Lin, Y.-W., Zhang, X., Chou, T.-C., Tsai, T.-J., Kapuriya, N., Kakadiya, R., & Su, T.-L. (2009). Synthesis and in vitro cytotoxicity of 9-anilinoacridines bearing N-mustard residue on both anilino and acridine rings. *European Journal of Medicinal Chemistry*, 44 (7), 3056-3059.
- Cheng, C.-C., & Yan, S.-J. (2004). *The Friedländer Synthesis of Quinolines*. *Organic Reactions*: John Wiley & Sons, Inc. 236-253.
- Comsa, E., Nguyen, K.-A., Loghin, F., Boumendjel, A., Peuchmaur, M., Andrieu, T., & Falson, P. (2018). Ovarian cancer cells cisplatin sensitization agents selected by mass cytometry target ABCC2 inhibition. *Future Medicinal Chemistry*, 10 (11), 1349-1360.
- Cutillas, N., Yellol, G. S., de Haro, C., Vicente, C., Rodríguez, V., & Ruiz, J. (2013). Anticancer cyclometalated complexes of platinum group metals and gold. *Coordination Chemistry Reviews*, 257 (19), 2784-2797.

- Dai, Y., Xu, K., Li, Q., Wang, C., Liu, X., & Wang, P. (2016). Acridine-based complex as amino acid anion fluorescent sensor in aqueous solution. *Spectrochimica Acta Part A: Molecular and Biomolecular Spectroscopy*, 157, 1-5.
- Das, S., & Thakur, A. J. (2011). A green development of Bernthsen 9-substituted acridine synthesis in the absence of solvent catalyzed by p-toluenesulphonic acid (p-TSA). *Green Chemistry Letters and Reviews*, 4 (2), 131-135.
- Dell' Amico, D. B., Via, L. D., García-Argáez, A. N., Labella, L., Marchetti, F., & Samaritani, S. (2015). Antiproliferative activity of platinum(II) complexes containing triphenylphosphine: Correlation between structure and biological activity. *Polyhedron*, 85, 685-689.
- Di Giorgio, C., Nikoyan, A., Decome, L., Botta, C., Robin, M., Reboul, J.-P., Sabatier, A.-S., Matta, A., & De Méo, M. (2008). DNA-damaging activity and mutagenicity of 16 newly synthesized thiazolo[5,4-a]acridine derivatives with high photo-inducible cytotoxicity. *Mutation Research/Genetic Toxicology and Environmental Mutagenesis*, 650 (2), 104-114.
- Ding, L., Yuan, F., Huang, L., Huang, J., Liu, X., & Liang, B. (2014). A novel fluorescence probe 9-(4-(1,2-diamine)benzene-N1-phenyl)acridine for nitric oxide determination. *Journal of Wuhan University of Technology-Material Science Edition*, 29 (4), 848-853.
- Eiter, L. C., Hall, N. W., Day, C. S., Saluta, G., Kucera, G. L., & Bierbach, U. (2009). Gold(I) Analogues of a Platinum–Acridine Antitumor Agent Are Only Moderately Cytotoxic but Show Potent Activity against Mycobacterium tuberculosis. *Journal of Medicinal Chemistry*, 52 (21), 6519-6522.
- Ellman, G. L. (1959). Tissue sulfhydryl groups. *Archives of Biochemistry and Biophysics*, 82 (1), 70-77.
- Fahrenholtz, C. D., Ding, S., Bernish, B. W., Wright, M. L., Zheng, Y., Yang, M., Yao, X., Donati, G. L., Gross, M. D., Bierbach, U., & Singh, R. (2016). Design and cellular studies of a carbon nanotube-based delivery system for a hybrid platinum-acridine anticancer agent. *Journal of Inorganic Biochemistry*, 165, 170-180.
- Gallego, C., Martínez, M., & Safont, V. S. (2007). Mechanism of the Competition between Phenyl Insertion and Ligand Reductive Elimination on a Hindered Platinum(IV) Cyclometalated Complex. *Organometallics*, 26 (3), 527-537.
- Gama, S., Mendes, F., Esteves, T., Marques, F., Matos, A., Rino, J., Coimbra, J., Ravera, M., Gabano, E., Santos, I., & Paulo, A. (2012). Synthesis and Biological Studies of Pyrazolyl-Diamine PtII Complexes Containing Polyaromatic DNA-Binding Groups. *A European Journal Chemical*, 13 (16), 2352-2362.
- Gamage, S. A., Figgitt, D. P., Wojcik, S. J., Ralph, R. K., Ransijn, A., Mauel, J., Yardley, V., Snowdon, D., Croft, S. L., & Denny, W. A. (1997). Structure– activity relationships for the antileishmanial and antitrypanosomal activities of 1'-substituted 9-anilinoacridines. *Journal of Medicinal Chemistry*, 40 (16), 2634-2642.

- Gao, H., Denny, W. A., Garg, R., & Hansch, C. (1998). Quantitative structure–activity relationships (QSAR) for 9-anilinoacridines: a comparative analysis. *Chemico-Biological Interactions*, 116 (3), 157-180.
- Garnier, T., Danel, M., Magné, V., Pujol, A., Bénéteau, V., Pale, P., & Chassaing, S. (2018). Copper(I)–USY as a Ligand-Free and Recyclable Catalyst for Ullmann-Type O-, N-, S-, and C-Arylation Reactions: Scope and Application to Total Synthesis. *The Journal of Organic Chemistry*, 83 (12), 6408-6422.
- Gensicka-Kowalewska, M., Cholewiński, G., & Dzierzbicka, K. (2017). Recent developments in the synthesis and biological activity of acridine/acridone analogues. *Royal Society Chemistry Advances*, 7 (26), 15776-15804.
- Giri, R., Goodell, J. R., Xing, C., Benoit, A., Kaur, H., Hiasa, H., & Ferguson, D. M. (2010). Synthesis and cancer cell cytotoxicity of substituted xanthenes. *Bioorganic & Medicinal Chemistry*, 18 (4), 1456-1463.
- Godino-Ojer, M., Martín-Aranda, R. M., Maldonado-Hódar, F. J., Pérez-Cadenas, A. F., & Pérez-Mayoral, E. (2018). Developing strategies for the preparation of Co-carbon catalysts involved in the free solvent selective synthesis of aza-heterocycles. *Molecular Catalysis*, 445, 223-231.
- Goodell, J. R., Madhok, A. A., Hiasa, H., & Ferguson, D. M. (2006). Synthesis and evaluation of acridine- and acridone-based anti-herpes agents with topoisomerase activity. *Bioorganic & Medicinal Chemistry*, 14 (16), 5467-5480.
- Guo, Q.-L., Su, H.-F., Wang, N., Liao, S.-R., Lu, Y.-T., Ou, T.-M., Tan, J.-H., Li, D., & Huang, Z.-S. (2017). Synthesis and evaluation of 7-substituted-5,6-dihydrobenzo[c]acridine derivatives as new c-KIT promoter G-quadruplex binding ligands. *European Journal of Medicinal Chemistry*, 130, 458-471.
- Hernán-Gómez, A., Herd, E., Uzelac, M., Cadenbach, T., Kennedy, A. R., Borilovic, I., Aromí, G., & Hevia, E. (2015). Zincate-Mediated Arylation Reactions of Acridine: Pre- and Postarylation Structural Insights. *Organometallics*, 34 (11), 2614-2623.
- Ibrahim, M. Y., Abdul, A. B., Ibrahim, T. A. T., Abdelwahab, S. I., Elhassan, M. M., & Syam, M. M. (2010). Evaluation of acute toxicity and the effect of single injected doses of zerumbone on the kidney and liver functions in Sprague Dawley rats. *African Journal of Biotechnology*, 9 (28), 4442-4450.
- Ibrahim, M. Y., Hashim, N. M., Mohan, S., Abdulla, M. A., Abdelwahab, S. I., Arbab, I. A., Yahayu, M., Ali, L. Z., & Ishag, O. E. (2015).  $\alpha$ -Mangostin from *Cratoxylum arborescens*: an in vitro and in vivo toxicological evaluation. *Arabian Journal of Chemistry*, 8 (1), 129-137.
- Jamali, S., Nabavizadeh, S. M., & Rashidi, M. (2008). Binuclear Cyclometalated Organoplatinum Complexes Containing 1,1'-Bis(diphenylphosphino)ferrocene as Spacer Ligand: Kinetics and Mechanism of MeI Oxidative Addition. *Inorganic Chemistry*, 47 (12), 5441-5452.

- Janočková, J., Plšíková, J., Kašpárková, J., Brabec, V., Jendželovský, R., Mikeš, J., Koval', J., Hamul'áková, S., Fedoročko, P., Kuča, K., & Kožurková, M. (2015). Inhibition of DNA topoisomerases I and II and growth inhibition of HL-60 cells by novel acridine-based compounds. *European Journal of Pharmaceutical Sciences*, 76, 192-202.
- Janovec, L., Kožurková, M., Sabolová, D., Ungvarský, J., Paulíková, H., Plšíková, J., Vantová, Z., & Imrich, J. (2011). Cytotoxic 3,6-bis((imidazolidinone)imino)acridines: Synthesis, DNA binding and molecular modeling. *Bioorganic & Medicinal Chemistry*, 19 (5), 1790-1801.
- Jia, C.-S., Zhang, Z., Tu, S.-J., & Wang, G.-W. (2006). Rapid and efficient synthesis of poly-substituted quinolines assisted by p-toluene sulphonic acid under solvent-free conditions: comparative study of microwave irradiation versus conventional heating. *Organic & Biomolecular Chemistry*, 4 (1), 104-110.
- Jimenez, M. B., Gonzalez, F. S., & Caballero, M. C. (2009). Crystal structure of dimethyl 5-(acridin-9-yloxy) isophthalate-methanol (1: 1), C<sub>23</sub>H<sub>17</sub>NO<sub>5</sub>· CH<sub>3</sub>OH. *Zeitschrift für Kristallographie-New Crystal Structures*, 224 (4), 603-604.
- Kalirajan, R., Muralidharan, V., Jubie, S., Gowramma, B., Gomathy, S., Sankar, S., & Elango, K. (2012). Synthesis of Some Novel Pyrazole-Substituted 9-Anilinoacridine Derivatives and Evaluation for their Antioxidant and Cytotoxic Activities. *Journal of Heterocyclic Chemistry*, 49 (4), 748-754.
- Kawasaki, M., Fuchigami, T., Kobashi, N., Nakagaki, T., Sano, K., Atarashi, R., Yoshida, S., Haratake, M., Nishida, N., & Nakayama, M. (2017). Development of radioiodinated acridine derivatives for in vivo imaging of prion deposits in the brain. *Bioorganic & Medicinal Chemistry*, 25 (3), 1085-1093.
- Ketron, A. C., Denny, W. A., Graves, D. E., & Osheroff, N. (2012). Amsacrine as a Topoisomerase II Poison: Importance of Drug-DNA Interactions. *American Chemical Society-Biochemistry*, 51 (8), 1730-1739.
- Kim, T. K., Kim, J. E., Youn, U. J., Han, S. J., Kim, I.-C., Cho, C.-G., & Yim, J. H. (2018). Total Syntheses of Lobaric Acid and Its Derivatives from the Antarctic Lichen *Stereocaulon alpinum*. *Journal of Natural Products*, 81 (6), 1460-1467.
- Kim, D.-Y., Kim, M., Shinde, S., Sung, J.-S., & Ghodake, G. (2017). Cytotoxicity and antibacterial assessment of gallic acid capped gold nanoparticles. *Colloids and Surfaces B: Biointerfaces*, 149, 162-167.
- Korth, C., May, B. C. H., Cohen, F. E., & Prusiner, S. B. (2001). Acridine and phenothiazine derivatives as pharmacotherapeutics for prion disease. *Proceedings of the National Academy of Sciences of the United States of America*, 98 (17), 9836-9841.
- Kumar, A., Kumar, A., Gupta, R. K., Paitandi, R. P., Singh, K. B., Trigun, S. K., Hundal, M. S., & Pandey, D. S. (2016). Cationic Ru(II), Rh(III) and Ir(III) complexes containing cyclic  $\pi$ -perimeter and 2-aminophenyl benzimidazole ligands: Synthesis, molecular structure, DNA and protein binding, cytotoxicity and anticancer activity. *Journal of Organometallic Chemistry*, 801, 68-79.

- Kumar, A., Kumar, N., Roy, P., Sondhi, S. M., & Sharma, A. (2015). Synthesis of acridine cyclic imide hybrid molecules and their evaluation for anticancer activity. *Medicinal Chemistry Research*, 24 (8), 3272-3282.
- Kumar, P., Kumar, R., & Prasad, D. N. (2013). Synthesis and biological evaluation of new 9-aminoacridine-4-carboxamide derivatives as anticancer agents: 1st Cancer Update. *Arabian Journal of Chemistry*, 6 (1), 59-65.
- Kumar, R., Sharma, A., Sharma, S., Silakari, O., Singh, M., & Kaur, M. (2017). Synthesis, characterization and antitumor activity of 2-methyl-9-substituted acridines. *Arabian Journal of Chemistry*, 10, S956-S963.
- Lang, X.-L., Sun, Q.-S., Chen, Y.-Z., Li, L.-L., Tan, C.-Y., Liu, H.-X., Gao, C.-M., & Jiang, Y.-Y. (2013). Novel synthetic 9-benzyloxyacridine analogue as both tyrosine kinase and topoisomerase I inhibitor. *Chinese Chemical Letters*, 24 (8), 677-680.
- Li, B., Gao, C.-M., Sun, Q.-S., Li, L.-L., Tan, C.-Y., Liu, H.-X., & Jiang, Y.-Y. (2014). Novel synthetic acridine-based derivatives as topoisomerase I inhibitors. *Chinese Chemical Letters*, 25 (7), 1021-1024.
- Liu, X.-Y., Liang, F., Ding, L., Li, Q., Jiang, Z.-Q., & Liao, L.-S. (2016). A new synthesis strategy for acridine derivatives to constructing novel host for phosphorescent organic light-emitting diodes. *Dyes and Pigments*, 126, 131-137.
- Lovejoy, K. S., & Lippard, S. J. (2009). Non-Traditional Platinum Compounds for Improved Accumulation, Oral Bioavailability, and Tumor Targeting. *Dalton Transactions* (48), 10651-10659.
- Lowry, O. H., Rosebrough, N. J., Farr, A. L., & Randall, R. J. (1951). Protein measurement with the Folin phenol reagent. *Journal of Biological Chemistry*, 193 (1), 265-275.
- Loza-Mejía, M. A., Castillo, R., & Lira-Rocha, A. (2009). Molecular modeling of tricyclic compounds with anilino substituents and their intercalation complexes with DNA sequences. *Journal of Molecular Graphics and Modelling*, 27 (8), 900-907.
- Martín, R., Crespo, M., Font-Bardia, M., & Calvet, T. (2009). Steric promotion in the cycloplatination of primary amines. *Polyhedron*, 28 (7), 1369-1373.
- Matesanz, A. I., Hernández, C., & Souza, P. (2014). New bioactive 2,6-diacetylpyridine bis(p-chlorophenylthiosemicarbazone) ligand and its Pd(II) and Pt(II) complexes: Synthesis, characterization, cytotoxic activity and DNA binding ability. *Journal of Inorganic Biochemistry*, 138, 16-23.
- Matesanz, A. I., Leitao, I., & Souza, P. (2013). Palladium(II) and platinum(II) bis(thiosemicarbazone) complexes of the 2,6-diacetylpyridine series with high cytotoxic activity in cisplatin resistant A2780cisR tumor cells and reduced toxicity. *Journal of Inorganic Biochemistry*, 125, 26-31.

- Medapi, B., Meda, N., Kulkarni, P., Yogeewari, P., & Sriram, D. (2016). Development of acridine derivatives as selective Mycobacterium tuberculosis DNA gyrase inhibitors. *Bioorganic & Medicinal Chemistry*, 24 (4), 877-885.
- Medici, S., Peana, M., Nurchi, V. M., Lachowicz, J. I., Crisponi, G., & Zoroddu, M. A. (2015). Noble metals in medicine: Latest advances. *Coordination Chemistry Reviews*, 284, 329-350.
- Mignon, P., Tiano, M., Belmont, P., Favre-Réguillon, A., Chermette, H., & Fache, F. (2013). Unusual reactivities of acridine derivatives in catalytic hydrogenation. A combined experimental and theoretical study. *Journal of Molecular Catalysis A: Chemical*, 371, 63-69.
- Mikata, Y., Yokoyama, M., Mogami, K., Kato, M., Okura, I., Chikira, M., & Yano, S. (1998). Intercalator-linked cisplatin: synthesis and antitumor activity of cis-dichloroplatinum(II) complexes connected to acridine and phenylquinolines by one methylene chain. *Inorganica Chimica Acta*, 279 (1), 51-57.
- Mitra, P., Chakraborty, P. K., Saha, P., Ray, P., & Basu, S. (2014). Antibacterial efficacy of acridine derivatives conjugated with gold nanoparticles. *International Journal of Pharmaceutics*, 473 (1), 636-643.
- Mochida, T., Torigoe, R., Koinuma, T., Asano, C., Satou, T., Koike, K., & Nikaido, T. (2006). Platinum-Group Chelate Complexes with 9-Hydroxyphenalenone Derivatives: Synthesis, Structures, Spectroscopic Properties and Cytotoxic Activities. *European Journal of Medicinal Chemistry*, 2006 (3), 558-565.
- Mondal, S. (2016). Recent advancement of Ullmann-type coupling reactions in the formation of C–C bond. *ChemTexts*, 2 (4), 17.
- Mondek, J., Mravec, F., Halasová, T., Hnylučová, Z., & Pekař, M. (2014). Formation and dissociation of the acridine orange dimer as a tool for studying polyelectrolyte–surfactant interactions. *Langmuir*, 30 (29), 8726-8734.
- Mukherjee, N., Podder, S., Banerjee, S., Majumdar, S., Nandi, D., & Chakravarty, A. R. (2016). Targeted photocytotoxicity by copper (II) complexes having vitamin B 6 and photoactive acridine moieties. *European Journal of Medicinal Chemistry*, 122, 497-509.
- Obrist, F., Michels, J., Durand, S., Chery, A., Pol, J., Levesque, S., Joseph, A., Astesana, V., Pietrocola, F., Wu, G. S., Castedo, M., & Kroemer, G. (2018). Metabolic vulnerability of cisplatin-resistant cancers. *The EMBO Journal*.
- Olszewska, P., Mikiciuk-Olasik, E., Błaszczak-Świątkiewicz, K., Szymański, J., & Szymański, P. (2014). Novel tetrahydroacridine derivatives inhibit human lung adenocarcinoma cell growth by inducing G1 phase cell cycle arrest and apoptosis. *Biomedicine & Pharmacotherapy*, 68 (8), 959-967.
- Pang, X., Chen, C., Su, X., Li, M., & Wen, L. (2014). Diverse Tandem Cyclization Reactions of o-Cyanoanilines and Diaryliodonium Salts with Copper Catalyst for the Construction of Quinazolinimine and Acridine Scaffolds. *Organic Letters*, 16 (23), 6228-6231.

- Pereira, E., do Quental, L., Palma, E., Oliveira, M. C., Mendes, F., Raposinho, P., Correia, I., Lavrado, J., Di Maria, S., Belchior, A., Vaz, P., Santos, I., & Paulo, A. (2017). Evaluation of Acridine Orange Derivatives as DNA-Targeted Radiopharmaceuticals for Auger Therapy: Influence of the Radionuclide and Distance to DNA. *Scientific Reports*, 7, 42544.
- Perez, S. A., de Haro, C., Vicente, C., Donaire, A., Zamora, A., Zajac, J., Kosthunova, H., Brabec, V., Bautista, D., & Ruiz, J. (2017). New Acridine Thiourea Gold(I) Anticancer Agents: Targeting the Nucleus and Inhibiting Vasculogenic Mimicry. *ACS Chemical Biology*.
- Popp, F. D. (1962). Polyphosphoric Acid in the Bernthsen Reaction. *The Journal of Organic Chemistry*, 27 (7), 2658-2659.
- Prajapati, S. P., Kaushik, N. K., Zaveri, M., Mohanakrishnan, D., Kawathekar, N., & Sahal, D. (2017). Synthesis, characterization and antimalarial evaluation of new  $\beta$ -benzoylstyrene derivatives of acridine. *Arabian Journal of Chemistry*, 10, S274-S280.
- Prajina, O., Thomas Muthiah, P., & Perdih, F. (2016). Supra-molecular inter-actions in a 1:1 co-crystal of acridine and 3-chloro-thio-phene-2-carb-oxy-lic acid. *Acta Crystallographica Section E: Crystallographic Communications*, 72 (Pt 5), 659-662.
- Ramachandran, E., Senthil Raja, D., Bhuvanesh, N. S., & Natarajan, K. (2012). Mixed ligand palladium(II) complexes of 6-methoxy-2-oxo-1,2-dihydroquinoline-3-carbaldehyde 4N-substituted thiosemicarbazones with triphenylphosphine co-ligand: synthesis, crystal structure and biological properties. *Dalton Transactions*, 41 (43), 13308-13323.
- Rubio-Pons, Ò., Serrano-Andrés, L., & Merchán, M. (2001). A theoretical insight into the photophysics of acridine. *The Journal of Physical Chemistry A*, 105 (42), 9664-9673.
- Saini, R., & Dharawath, N. (2018). Friedlander synthesis of highly functionalized isoxazolyl quinoline libraries via addition of C(sp<sup>3</sup>)–H bond to aldehydes. *Journal of the Iranian Chemical Society*.
- Sambiagio, C., Marsden, S. P., Blacker, A. J., & McGowan, P. C. (2014). Copper catalysed Ullmann type chemistry: from mechanistic aspects to modern development. *Chemical Society Reviews*, 43 (10), 3525-3550.
- See, I., Ee, C. G., Teh, S. S., Kadir, A. A., & Daud, S. (2014). Two New Chemical Constituents from the Stem Bark of *Garcinia mangostana*. *Molecules*, 19 (6).
- Solovyeva, E. V., Starova, G. L., Myund, L. A., & Denisova, A. S. (2016). X-ray, IR and Raman study of Ag (I), Cu (II) and Cd (II) complexes with 4, 5-bis (N, N-di (2-hydroxyethyl) iminomethyl) acridine. *Polyhedron*, 106, 1-9.
- Sondhi, S. M., Kumar, S., Rani, R., Chakraborty, A., & Roy, P. (2013). Synthesis of Bis-acridine Derivatives Exhibiting Anticancer and Anti-inflammatory Activity. *Journal of Heterocyclic Chemistry*, 50 (2), 252-260.

- Sondhi, S. M., Singh, J., Rani, R., Gupta, P. P., Agrawal, S. K., & Saxena, A. K. (2010). Synthesis, anti-inflammatory and anticancer activity evaluation of some novel acridine derivatives. *European Journal of Medicinal Chemistry*, 45 (2), 555-563.
- Souibgui, A., Gaucher, A., Marrot, J., Bourdreux, F., Aloui, F., Ben Hassine, B., & Prim, D. (2014). New series of acridines and phenanthrolines: synthesis and characterization. *Tetrahedron*, 70 (18), 3042-3048.
- Sun, Y., Xu, G., Cao, Z., & Gou, S. (2013). Synthesis and biological evaluation of platinum(II) complexes containing (1R,2R)-N1-alkyl-1,2-diaminocyclohexane and D-(+)-camphorate ligands. *Inorganica Chimica Acta*, 395, 154-159.
- Teimouri, A., & Chermahini, A. N. (2016). A mild and highly efficient Friedländer synthesis of quinolines in the presence of heterogeneous solid acid nano-catalyst. *Arabian Journal of Chemistry*, 9, S433-S439.
- Temple, M. D., Recabarren, P., McFadyen, W. D., Holmes, R. J., Denny, W. A., & Murray, V. (2002). The interaction of DNA-targeted 9-aminoacridine-4-carboxamide platinum complexes with DNA in intact human cells. *Biochimica et Biophysica Acta (BBA) - Gene Structure and Expression*, 1574 (3), 223-230.
- Valdés, A. F.-C. (2011). Acridine and acridinones: old and new structures with antimalarial activity. *The Open Medicinal Chemistry Journal*, 5, 11-20.
- Wainwright, M. (2001). Acridine—a neglected antibacterial chromophore. *Journal of Antimicrobial Chemotherapy*, 47 (1), 1-13.
- Wang, Z. (2010). *Friedländer Condensation Comprehensive. Organic Name Reactions and Reagents*: John Wiley & Sons, Inc.
- Wybenga, D. R., Pileggi, V. J., Dirstine, P. H., & Di Giorgio, J. (1970). Direct manual determination of serum total cholesterol with a single stable reagent. *Clinical Chemistry*, 16 (12), 980-984.
- Yang, Z.-M., Huang, J., Qin, J.-K., Dai, Z.-K., Lan, W.-L., Su, G.-F., Tang, H., & Yang, F. (2014). Design, synthesis and biological evaluation of novel 1-hydroxyl-3-aminoalkoxy xanthone derivatives as potent anticancer agents. *European Journal of Medicinal Chemistry*, 85 (Supplement C), 487-497.
- Zhang, Y., Pan, J., Zhang, G., & Zhou, X. (2015). Intercalation of herbicide propyzamide into DNA using acridine orange as a fluorescence probe. *Sensors and Actuators B: Chemical*, 206 (Supplement C), 630-639.
- Zhao, J., Gou, S., Xu, G., & Cheng, L. (2014). Antitumor platinum(II) complexes of N-monoalkyl 1R,2R-diamino-cyclohexanes with 3-(nitrooxy)cyclobutane-1,1-dicarboxylate as a leaving group. *European Journal of Medicinal Chemistry*, 85, 408-417.
- Zhao, D., Krause, J. A., & Connick, W. B. (2015). Platinum(II) Monomer and Dimer Complexes with a Bis(oxazoliny)phenyl Pincer Ligand. *Inorganic Chemistry*, 54 (17), 8339-8347.

## LIST OF PUBLICATIONS AND PAPER PRESENTED

### List of Publication:

Ismail, N. A., Salman, A. A., Yusof, M. S. M., Soh, S. K. C., Mohd, H. A., & Sarip, R. (2018). The synthesis of a novel anticancer compound, N-(3,5 dimethoxyphenyl) acridin-9-amine and evaluation of its toxicity. *Open Chemistry Journal*, 5, 32-43.

### Presentation:

Nur Amajeida binti Ismail, Synthesis, Characterization and Biological Activities of Acridine Derivatives. International Conference in Organic Synthesis 2016, Sarawak, Malaysia, 21-24 August 2016.

University of Malaya